International Journal of Nanomedicine

Dovepress
open access to scientific and medical research

Open Access Full Text Article

ORIGINAL RESEARCH

Surface biofunctionalized CdS and ZnS quantum dot nanoconjugates for nanomedicine and oncology: to be or not to be nanotoxic?

This article was published in the following Dove Press journal:
International Journal of Nanomedicine
14 September 2016
Number of times this article has been viewed

Alexandra AP Mansur[1]
Herman S Mansur[1]
Sandhra M de Carvalho[1–3]
Zélia IP Lobato[2]
Maria IMC Guedes[2]
Maria F Leite[3]

[1]Center of Nanoscience, Nanotechnology, and Innovation-CeNano[2]I, Department of Metallurgical and Materials Engineering, [2]Department of Preventive Veterinary Medicine, Veterinary School, [3]Department of Physiology and Biophysics, ICB, Federal University of Minas Gerais, Belo Horizonte, MG, Brazil

Abstract: Herein, for the first time, we demonstrated that novel biofunctionalized semiconductor nanomaterials made of Cd-containing fluorescent quantum dot nanoconjugates with the surface capped by an aminopolysaccharide are not biologically safe for clinical applications. Conversely, the ZnS-based nanoconjugates proved to be noncytotoxic, considering all the parameters investigated. The results of in vitro cytotoxicity were remarkably dependent on the chemical composition of quantum dot (CdS or ZnS), the nature of the cell (human cancerous and embryonic types), and the concentration and time period of exposure to these nanomaterials, caused by the effects of Cd^{2+} on the complex nanotoxicity pathways involved in cellular uptake. Unexpectedly, no decisive evidence of nanotoxicity of CdS and ZnS conjugates was observed in vivo using intravenous injections in BALB/c mice for 30 days, with minor localized fluorescence detected in liver tissue specimens. Therefore, these results proved that CdS nanoconjugates could pose an excessive threat for clinical applications due to unpredicted and uncorrelated in vitro and in vivo responses caused by highly toxic cadmium ions at biointerfaces. On the contrary, ZnS nanoconjugates proved that the "safe by design" concept used in this research (ie, biocompatible core–shell nanostructures) could benefit a plethora of applications in nanomedicine and oncology.

Keywords: fluorescent nanoparticles, semiconductor quantum dots, nanotoxicity, bionanoconjugates, nanoprobes

Introduction

There is nearly a consensus among scientists and professionals that heavy metals such as cadmium, lead, and mercury ions are extremely toxic to animals and humans, with severe hazardous effects to the entire environment. In addition, regarding the toxicity at the nano scale, referred to as nanotoxicity, these harmful characteristics can be potentially boosted due to the extremely high surface-to-volume ratio, which exponentially increases the number of surface molecules and undercoordinated atoms exposed to interact with the microdomain.[1–5] Despite the remarkable advances in the development of fluorescent colloidal semiconductor nanocrystals, known as quantum dots (QDs), in the recent decades, mostly driven by their unique optical, magnetic, and electronic properties, the large majority are predominantly produced using Cd-based semiconductor core (CdX, X=S, Se, Te) with some type of surface functionalization aiming at their potential applications in the biomedical and pharmaceutical fields.[3] However, some researchers are convinced that heavy metal-based QDs (eg, Cd, Pb, and Hg) will never achieve biomedical and clinical applications as they inherently carry a highly toxic core, which would behave unpredictably in the living body.[3,5] Moreover, the

Correspondence: Herman S Mansur
Center of Nanoscience, Nanotechnology, and Innovation-CeNano[2]I, Department of Metallurgical and Materials Engineering, Federal University of Minas Gerais, Av Antônio Carlos, 6627, School of Engineering, 31270-901, Belo Horizonte, MG, Brazil
Tel +55 31 3409 1843
Fax +55 31 3409 1815
Email hmansur@demet.ufmg.br

submit your manuscript | www.dovepress.com
Dovepress
http://dx.doi.org/10.2147/IJN.S115208

use of toxic reagents with organometallic precursors at high temperatures for producing QDs is increasingly raising environmental concerns from researchers and regulators, demanding safer and more eco-friendly processes from scientists. In this sense, the cytotoxicity of QDs is highly controversial, with many imperative questions remaining unanswered and without a definitive solution for a reliable clinical application in nanomedicine yet. Several articles and interesting reviews have recently been published addressing the toxicity of QDs using in vitro bioassays with different cell lines and in vivo tests with small animal models.[6,7] A well-designed pioneering study was performed by Ye et al,[8] which indicated that Cd-based QDs encapsulated in phospholipid micelles did not show evidence of toxicity when intravenously injected into nonhuman primates after 90 days of monitoring. Thus, the noteworthy inconsistency in the toxicological data reported from in vitro and in vivo studies is mostly associated with the fact that QDs and other nanomaterials are fundamentally different, despite sharing some similarities in the chemical composition and preparation methods.

The most comprehensive compiled study so far of Cd-containing QDs has just been published in *Nature Nanotechnology* by Medintz's research group.[9] Herein, the authors conducted a meta-analysis of cellular toxicity using >300 articles, where they reported subgroups with clearly correlated attributes but others with no apparent correlation. Therefore, it is unquestionably a rather complex coupling of attributes regarding the toxicity response of cells toward Cd-based QDs that poses great challenges for creating a generalized cause–effect relationship.[10]

In this sense, the development of novel functional semiconductor nanomaterials for targeting biomedical and pharmaceutical applications requires a more in-depth knowledge of the complex interactions taking place at the nanomaterial biointerface. Understanding these interactions and their consequences is of fundamental importance for the identification of potential paradigms of nanotoxicity.[11] This approach is a starting point for appropriately assessing the cytotoxicity and biocompatibility of QDs toward designing and producing biologically and environmentally safer nanomaterials.[5]

To minimize or eventually exclude the potential toxicity associated with the use of heavy metals in QDs, the interest in alternative semiconductors made of zinc chalcogenides (eg, ZnX, X=S, Se, Te) and Zn-doped compounds (eg, Mn^{2+}, Fe^{3+}, Cu^{+}, Ni^{2+}) has intensified in recent years for producing nontoxic and environmentally friendly nanomaterials.[3,12] Some studies have reported the use of a ZnS layer on a Cd-based core as a protective layer against the degradation of the core, which may potentially cause the release of toxic Cd^{2+} species in the biological environment under in vivo applications. From the toxicity perspective, the most common strategy used is the biofunctionalization of QDs with capping ligands for rendering them water soluble and biocompatible for biomedical applications, which may theoretically protect the hazardous heavy metal semiconductor core with an organic biocompatible layer.[2,3,13,14] In this sense, some biomolecules such as carbohydrates,[15,16] peptides,[17] amino acids,[18] enzymes, and proteins[19] play a key role because they simultaneously combine the functional groups with the biological affinity for the specific targeting for cell bioimaging, detection and diagnosis, and drug carriers.[3,20] More recently, aminopolysaccharides such as chitosan (CHI) and its derivatives have been investigated as a very interesting choice for the biofunctionalization of QDs, due to their usual biocompatibility, reasonable water solubility, chemical stability against degradation, environmental compatibility, and abundance as a semi-processed product obtained from natural sources (eg, chitin extracted from crustacean exoskeletons).[13,21] Nonetheless, besides the surface functionalization of the conjugated system, the overall cell behavior and the nanotoxicological response of the living organism are significantly governed by the nanoparticle size, surface characteristics such as hydrophobicity and charge, steric hindrance, chemical functional groups, and biochemical affinities at the biointerfaces.[5,22,23]

Despite the great interest in understanding the nanotoxicity of QDs,[3] a systematic and comprehensive investigation comparing the cytotoxicity responses and the complex mechanisms comprising QD-based nanoconjugates made of Cd-based (toxic) and Zn-based (nontoxic) cores and surface functionalization by aminopolysaccharides was not found in the consulted literature.

In this study, it is hypothesized that water-soluble CdS and ZnS QD nanoconjugates biofunctionalized with biopolymer ligands present distinct nanotoxicity patterns using an in vitro assay toward three cell types and an in vivo assay with mice as animal model. It was proven that the CdS heavy metal core determined the cytotoxic responses, which were strongly dependent on the concentration, time of exposure, and cell type. On the other hand, ZnS nanoconjugates were found to be nontoxic under all conditions investigated.

Material and methods

Synthesis and characterization of nanoconjugates

All of the reagents and precursors, including cadmium perchlorate hydrate (Sigma-Aldrich, St Louis, MO, USA,

$Cd(ClO_4)_2 \cdot 6H_2O$), zinc chloride (Sigma-Aldrich, 98%, $ZnCl_2$), sodium sulfide (Synth, Sao Paulo, Brazil, >98%, $Na_2S \cdot 9H_2O$), sodium hydroxide (NaOH, 99%; Merck, Darmstadt, Germany), and acetic acid (Synth, Brazil, ≥99.7%, CH_3COOH were used as received. Low molecular weight (LM_W) chitosan powder (catalogue #448869, M_W =60–70 kDa; degree of deacetylation =96.1%; viscosity =35 cPoise, 1 wt% in 1% acetic acid; Sigma-Aldrich) was used simultaneously as capping ligand and surface functionalization of QDs.

A chitosan acetate solution (1%, w/v) was prepared by adding chitosan powder (0.5 g) to a 50 mL aqueous solution (2%, v/v) of acetic acid and stirring at room temperature until complete solubilization occurred (pH ~3.6). CdS and ZnS colloidal nanoparticles stabilized by chitosan (CHI) were synthesized *via* a "green" aqueous processing route in a reaction flask at room temperature (RT) as follows: 2 mL of chitosan solution and 45 mL of DI-water were added to the flask reacting vessel and the pH was adjusted to 6.0±0.1 with NaOH (0.1 mol·L^{-1}). Under moderate magnetic stirring, 4.0 mL of the metal (Cd^{2+} or Zn^{2+}) precursor solution ($Cd(ClO_4)_2 \cdot 6H_2O$, 8×10^{-3} mol·L^{-1} or $ZnCl_2$, 8×10^{-3} mol·L^{-1}) and 2.5 mL of the S_2- precursor solution ($Na_2S \cdot 9H_2O$, 1.0×10^{-2} mol·L^{-1}) were added to the flask (the S:Cd molar ratio was kept at 1:2) and stirred for 10 min. The QD colloidal dispersions produced were clear, stable and homogeneous. The QD colloids were 2 dialyzed for 24 h (with water changes after 2 h and 4 h) against 3 L of DI water using a Pur-A-Lyzer™ Mega Dialysis Kit (Sigma-Aldrich, cellulose membrane with molecular weight cut-off filter, MWCO of 12,000 Da) under moderate stirring at room temperature. After purification, the QD dispersions were stored at RT until further use. Unless specified otherwise, deionized water (Simplicity™; EMD Millipore, Billerica, MA, USA) with a resistivity of 18 MΩ·cm was used to prepare the solutions, and the procedures and analysis were performed at room temperature (23°C±2°C).

The synthesis of ZnS and CdS nanoconjugates followed a similar procedure reported by our group,[3] which is summarized in the Supplementary materials.

Ultraviolet–visible spectroscopy measurements were performed using a Perkin-Elmer equipment (Lambda EZ-210) in transmission mode. All the experiments were conducted in triplicate (n=3) unless specifically noted, and the data were presented as mean ± standard deviation.

The photoluminescence characterization of the CdS and ZnS nanoconjugates was conducted based on spectra acquired using a violet diode laser module at λ_{exc}=405 nm (150 mW; Roithner LaserTechnik GmbH, Vienna, Austria) coupled to a USB4000-VIS-NIR spectrophotometer (Ocean Optics, Dunedin, Fl, USA). All the tests were performed using a minimum of four repetitions (n≥4). Quantum yield was measured according to the established procedure using Rhodamine 6G (Sigma-Aldrich Co., St Louis, MO, USA) in ethanol as the standard at $\lambda_{excitation}$=405 nm.[24]

Nanostructural characterization of the QDs, based on the images and electron diffraction (ED) patterns, was obtained using a Tecnai G2-20-FEI transmission electron microscope (TEM) at an accelerating voltage of 200 kV. In all the TEM analyses, the samples were prepared by dropping the colloidal dispersion on a porous carbon grid. The QD size and size-distribution data were obtained based on the TEM images by measuring at least 100 randomly selected nanoparticles using image processing program (ImageJ, Version 1.50, public domain; National Institutes of Health).

X-ray photoelectron spectroscopy analysis was performed on an Amicus spectrometer (Kratos Analytical Ltd, Manchester, UK) using Mg·Kα as the excitation source. All peaks positions were corrected based on C 1s binding energy (284.6 eV).

Dynamic light scattering (DLS) and zeta potential or ζ-potential (ZP) analyses were performed using a Brookhaven ZetaPlus instrument with a laser light wavelength of 660 nm (35-mW red diode laser). The samples were measured at 25°C±2°C, and light scattering was detected at 90°. For the DLS measurements, the colloidal solutions of QDs (3 mL) were filtered three times through a 0.45 µm aqueous syringe filter (Millex LCR 25 mm; EMD Millipore) to remove any possible unwanted particles. Five measurements were performed for each system and averaged. ZP measurements were performed on the QD colloidal aqueous solutions using the laser Doppler electrophoresis technique. All the tests were performed using a minimum of ten replicates (n≥10), and the values were averaged.

Biological characterization of QD nanoconjugates

For biological assays, stock solutions of 1.0 µmol·L^{-1} of colloidal CdS and ZnS nanoconjugates were dispersed in cell culture media to final concentrations of 10 nmol·L^{-1} (1%), 50 nmol·L^{-1} (5%), and 100 nmol·L^{-1} (10%) for 3-(4,5-dimethylthiazol-2yl) 2,5-diphenyl tetrazolium bromide (MTT) experiments and 500 nmol·L^{-1} (50%) for cellular uptake analyses.

Cell cultures

The immortalized human osteosarcoma-derived (SAOS) cells were kindly provided by Professor A Goes of the

Department of Immunology and Biochemistry, Federal University of Minas Gerais. The derivative of human embryonic kidney 293 cells (HEK293T) was provided by Professor MF Leite of the Department of Physiology and Biophysics, UFMG. The SAOS and HEK293T cells were cultured in Dulbecco's Modified Eagle's Medium (DMEM) with 10% fetal bovine serum (FBS), streptomycin sulfate (10 mg·mL^{-1}), penicillin G sodium (10 units·mL^{-1}), and amphotericin b (0.025 mg·mL^{-1}); all of them were supplied by Thermo Fisher Scientific (Waltham, MA, USA), using a humidified atmosphere of 5% CO_2 at 37°C.

Human lymphoma cell line (Toledo CRL2631) was purchased from the Rio de Janeiro Cell Bank (BCRJ, Brazil). The cells were cultured in Roswell Park Memorial Institute Medium (RPMI 1640) with 10% FBS, streptomycin sulfate (10 mg·mL^{-1}), penicillin G sodium (10 units·mL^{-1}), and amphotericin b (0.025 mg·mL^{-1}); all of them were supplied by Thermo Fisher Scientific, in a humidified atmosphere of 5% CO_2 at 37°C.

Cytotoxicity assays

All the biological tests were conducted according to ISO 10993-5:2009 (biological evaluation of medical devices: tests for in vitro cytotoxicity).

MTT assay using 3-(4,5-dimethylthiazol-2yl) 2,5-diphenyl tetrazolium bromide

SAOS cells on passage 15, HEK293T cell on passage 11, and Toledo cells on passage 16 were plated (3×10^4 cells/well) in 96-well plates. Cell populations were synchronized in serum-free media for 24 hours. After that, for SAOS and HEK293T cells, the media volume was suctioned and replaced with DMEM containing 10% FBS for 24 hours. For Toledo cells, the medium volume was suctioned, centrifuged, and resuspended in the original medium containing 10% FBS. The samples of CdS and ZnS QD colloidal solutions were added to individual wells at final concentrations of 1% (10 nmol·L^{-1}), 5% (50 nmol·L^{-1}), and 10% (100 nmol·L^{-1}). Controls had been used with cells and DMEM (SAOS and HEK293T) or RPMI 1640 medium with 10% FBS, Triton X-100 (1%; Sigma-Aldrich Co.) as positive control, and chips of sterile polypropylene (1 mg·mL^{-1}; Eppendorf, Hamburg, Germany) as negative control. After 72 hours (3 days), 120 hours (5 days), and 168 hours (7 days), all media were aspirated and replaced with 60 µL of culture media containing serum in each well and photographed using an inverted optical microscope (Leica DM IL LED; Leica Microsystems, Wetzlar, Germany). MTT (5 mg·mL^{-1}; Sigma-Aldrich Co.) was added to each well and incubated for 4 hours in an oven at 37°C and 5% CO_2. Next, 40 µL of sodium dodecyl sulfate (Sigma-Aldrich Co.) solution/4% HCl was placed in each well and incubated for 16 hours in an oven at 37°C and 5% CO_2. Then, 100 µL were removed from each well and transferred to a 96-well plate. The absorbance was measured at 595 nm on iMark™ Microplate Absorbance Reader (Bio-Rad Laboratories Inc., Hercules, CA, USA) with a 595-nm filter. Percentage cell viability was calculated according to Equation 1. The values of the controls (wells with cells and no samples) were set to 100% cell viability.

$$\text{Cell viability} = \frac{\text{Abs of sample and cells}}{\text{Abs of control}} \times 100\% \quad (1)$$

Live/Dead™ assay

The SAOS cells on passage 16 were plated (3×10^4 cells/well) in 96-well plates. The cell populations were synchronized in serum-free medium for 24 hours, after which the medium was aspirated and replaced with medium containing 10% FBS. The CdS and ZnS nanoconjugate samples were added to the cells at concentrations of 1% and 5% for 72 hours. The reference controls were cells cultured in DMEM with 10% FBS. After 72 hours, all the media were aspirated and the cells were washed two times with 10 mL of phosphate-buffered saline (PBS; Thermo Fisher Scientific). The SAOS cells were treated with the Live/Dead™ Viability/Cytotoxicity Kit (Life Technologies of Brazil Ltd, São Paulo, Brazil) for 30 minutes, according to the manufacturer's specifications. Images of fluorescent emissions were separately acquired, calcein at 530±12 nm and ethidium homodimer-1 at 645±20 nm, with a Zeiss LSM Meta 510 confocal microscope (Carl Zeiss Meditec AG, Jena, Germany) and with an inverted optical microscope (Leica DM IL LED).

Cellular uptake of QD nanoconjugates

For the cellular uptake evaluation, SAOS cells on passage 45, HEK293T cell on passage 5, and Toledo cells on passage 18 were plated (5×10^4 cells/well) in 24-well plate. The cells were incubated for 4 days in 5% CO_2 at 37°C and synchronized for 24 hours. The CdS and ZnS QD nanoconjugates containing 50% of the medium solution (DMEM, for SAOS and HEK293T cells, or RPMI 1640, for Toledo cells), at a final concentration of 500 nmol·L^{-1} of QD nanoconjugates, were added to the cells. Next, the cells were incubated in 5% CO_2 at 37°C for 1 hour and washed with PBS (Thermo Fisher Scientific).

Quantitative flow cytometry analysis

For the flow cytometry analysis, Toledo cells were incubated with the QD-conjugate solutions as previously described and fixed with paraformaldehyde (3.7%) for 15 minutes. After washing with PBS (three times), the cells were suspended in PBS for cytometry analysis. A flow cytometer (BD FACSCanto™ II; BD Biosciences, San Jose, CA, USA) equipped with a 405-nm violet laser was used to analyze size (forward scatter) and granularity (side scatter). A laser at 488 nm was chosen to excite the QDs, and the fluorescence emissions were detected in the fluorescein isothiocyanate (FITC) channel. For the control, Toledo cells cultured with only RPMI 1640 medium with 10% FBS were analyzed. In addition, Toledo cells cultured with 50% of the medium solution and 50% of CHI solution, at the same concentration presented in QD dispersions (sample referred to as CHI), were evaluated (minimum of 2×10^4 cells from each sample were analyzed).

Endocytosis assay

For the endocytosis experiments, SAOS, HEK293T, and Toledo cells were incubated with the QD-conjugate solutions as previously described. In the sequence, the cells were fixed with paraformaldehyde (4%) for 30 minutes and washed three times with PBS and cover slips were mounted with Hydromount (Thermo Fisher Scientific). Confocal laser scanning fluorescence microscope (Zeiss LSM Meta 510), with a 488 nm argon laser irradiation to excite the QD associated with cells, was used to detect the fluorescence. The emissions were collected in the range between 505 nm and 530 nm. For the control, cells were incubated with only the original medium with 10% FBS (autofluorescence).

In vivo studies

All the animal experiments and protocols were approved by the animal ethics committee of Federal University of Minas Gerais (Project CETEA-UFMG/Nr#169/2014) and followed the guidelines of the Conselho Nacional de Controle de Experimentação Animal (CONCEA)-Brazilian law (n.º 11.794, 08 october, 2008). Animal injection and weight measurements of BALB/c mice were performed and handled at the Veterinary School, UFMG.

Fifteen male BALB/c mice, at 6 weeks of age and body weight ~20–30 g, were obtained from the Bioterism Center of UFMG. The animals were weighed, randomly divided into five homogenous groups, and were housed in cages. All animals were fed with water and standard commercial chow ad libitum. The experimental groups were divided as described in Table 1.

The mice were injected at first, sixth, and 22nd days of experiment with 200 µL of CHI solution dissolved in PBS (concentration of 20% in PBS) or QD colloidal dispersions (concentration of 40% in PBS or pure QD dispersion, 100%) via tail vein injection.

Animals were weighed and monitored for clinical signs every other day for 30 days. After 30 days, mice were euthanized by anesthetic overdose, and liver, spleen, and kidney samples were collected. The parts of the organ were fixed in 10% buffered formalin for further histological examination, and the parts were used for fluorescence analysis. Images and fluorescence profiles were obtained using Eclipse Ti-U inverted microscope (Nikon Instruments, Melville, NY, USA) coupled to a refrigerated CCD camera (DS-Qi1-U3, Nikon Instruments), FITC filter cube (excitation filter: 460–500 nm and emission filter: 510–560 nm), and imaging software NIS-Elements (Nikon Instruments; conditions: FTIC filter, N/D lamp control: 1, exposure time: 60 seconds, auto gain: 1.7×). For histology, tissue samples were embedded in paraffin, sectioned, stained with hematoxylin and eosin and examined by light microscopy (Nikon Eclipse E200; Nikon Instruments).

Statistical analysis

In this study, Prism software (GraphPad Software, Inc., La Jolla, CA, USA) was used for data analysis. Statistical significance was tested using one-way analysis of variance followed by Bonferroni's method. A P-value <0.05 was considered statistically significant. The experiments were performed at least in triplicate ($n\geq3$).

Table 1 Experimental groups distributed according to the type, concentration and the route of inoculation

Group	Inoculum	Concentration (final concentration)	Route	Sample identification
1	CdS QDs dispersion (1.0 µmol·L^{-1})	100% of QDs dispersion (1.0 µmol·L^{-1})	Intravenously (IV)	CdS 100% IV
2	CdS QDs dispersion (1.0 µmol·L^{-1})	40% of QDs dispersion in PBS (0.4 µmol·L^{-1})	Intravenously (IV)	CdS 40% IV
3	ZnS QDs dispersion (1.0 µmol·L^{-1})	100% of QDs dispersion (1.0 µmol·L^{-1})	Intravenously (IV)	ZnS 100% IV
4	ZnS QDs dispersion (1.0 µmol·L^{-1})	40% of QDs dispersion in PBS (0.4 µmol·L^{-1})	Intravenously (IV)	ZnS 40% IV
5 (control)	Chitosan solution (1.0 µmol·L^{-1})	20% of chitosan solution dissolved in PBS (0.2 µmol·L^{-1})	Intravenously (IV)	CHI 20% IV

Abbreviations: QDs, quantum dots; PBS, phosphate buffered saline; CHI, chitosan; IV, intravenously.

Results and discussion

Physicochemical characterization of QD–CHI nanoconjugates

In the UV–Vis spectra of CdS (Figure 1Aa) and ZnS (Figure 1Ba) stabilized with CHI, first excitonic transitions (λ_{exc}) were detected at 420±5 nm and 304±5 nm, respectively, "blue shifted" to bulk values (512 nm for CdS and 343 nm for ZnS),[25] indicating the formation of QDs in aqueous colloidal solution. The band gap energies (E_{QD}) estimated using the linear form of Tauc relation[26] were 2.74±0.02 eV and 3.86±0.02 eV for CdS and ZnS nanoconjugates, respectively (Figure 2). As expected for nanoparticles in the quantum

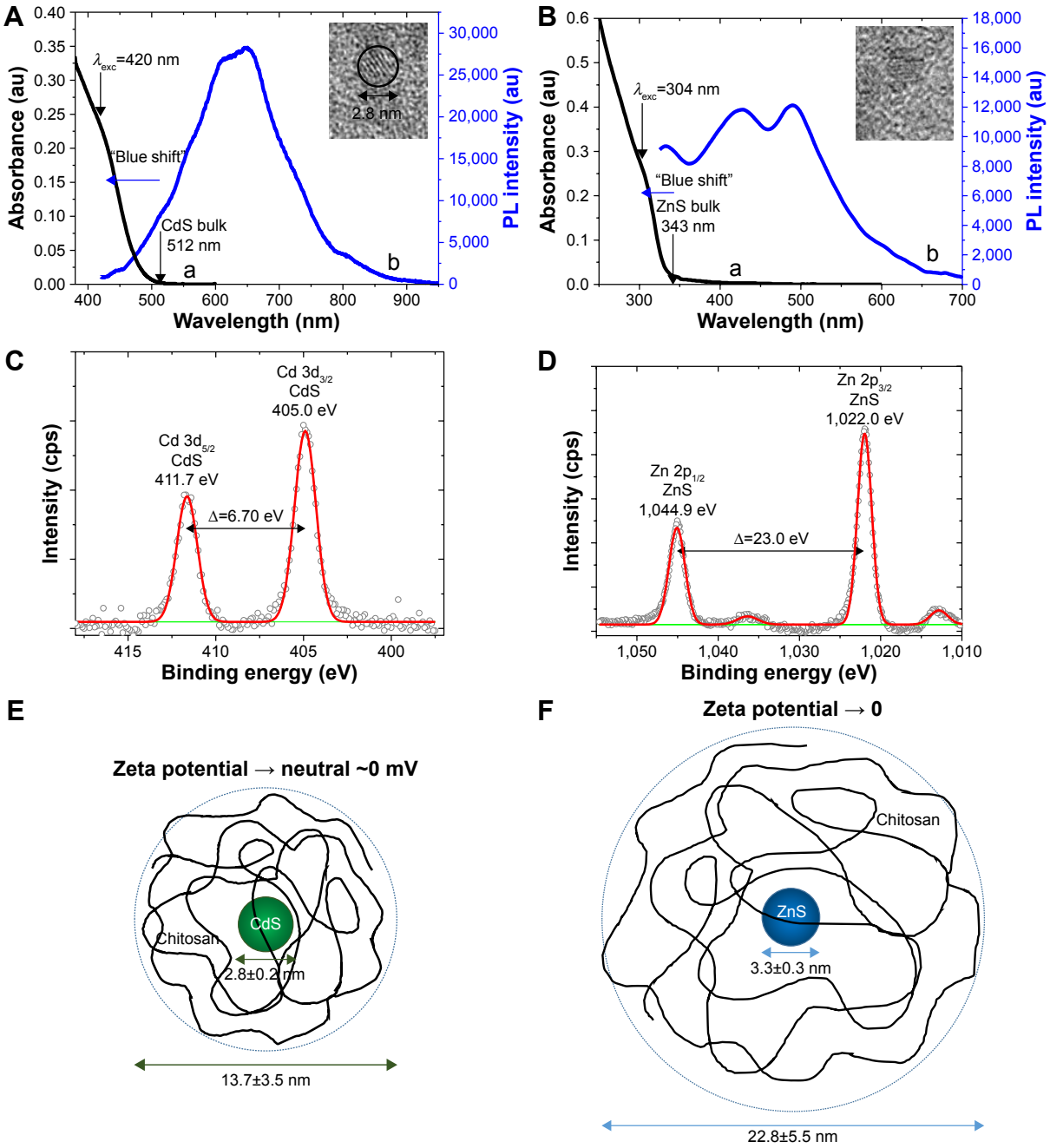

Figure 1 Physico-chemical characterization of CdS and ZnS quantum dots.

Notes: UV–Vis (a) and PL (b) spectra of CdS (**A**) and ZnS (**B**) QD colloidal dispersions. Inset: TEM image with the typical QD size diameter and nanocrystal lattice fringes. XPS spectra of Cd 3d region (**C**) for CdS nanoconjugates and Zn 2p region (**D**) for ZnS nanoconjugates. Schematic representation of QD size (diameter estimated with UV–Vis spectroscopy), HD, and ZP for CdS (**E**) and ZnS (**F**).

Abbreviations: UV–Vis, ultraviolet–visible; PL, photoluminescence; QD, quantum dot; TEM, transmission electron microscopy; XPS, X-ray photoelectron spectroscopy; HD, hydrodynamic diameter; ZP, zeta potential; λ_{exc}, wavelength of excitonic absorption; nm, nanometer; au, arbitrary unit; cps, counts per second; Δ, spin-orbit separation; eV, electron volt.

confinement regime, these band gap values are higher than the reference bulk value (E_g) of 2.42 eV and 3.61 eV[25] for CdS and ZnS, respectively, being the difference ($\Delta E = E_{QD} - E_g$) referred to as blue shift. The average CdS nanoparticle size ($2R$=2.8±0.2 nm) was determined using Henglein's empirical model,[27] which relates the diameter of the CdS nanoparticle ($2R$) to the exciton absorption transition onset (λ_{exc}). The average size of 3.3±0.3 nm for the ZnS nanocrystals was estimated using the empirical model,[28] which relates the nanoparticle size (r) to the optical band gap (E_{QD}).

These results were validated by the TEM analysis as shown in Figure 3. The histograms of the size distribution of CdS and ZnS QDs indicate monodisperse distributions with an average diameter of 3.1±0.3 nm and 3.2±0.4 nm, respectively. Lattice fringes were observed for both nanoparticles, indicating an ordered crystalline structure with an interplanar distance of ~0.33±0.02 nm for CdS and 0.31±0.02 nm for ZnS QDs, which is compatible with the (111) plane of cubic CdS (JCPDS 89-0440) and cubic ZnS (JCPDS 05-0566).

The photoluminescence spectra demonstrated that both semiconductor nanocrystal conjugates showed photoluminescent behavior under irradiation, with maxima wavelengths at ~50 nm and 500 nm for CdS (Figure 1Ab) and ZnS (Figure 1Bb), respectively. In both cases, band edge (excitonic transition) emissions were not detected and the radiative emissions were associated with point and surface defects.[29,30] The quantum yield of the CdS and ZnS nanoconjugates was estimated to be ~1% and 2%, respectively, which is in good agreement with reports published about QDs synthesized using low temperatures and aqueous colloidal routes.[31]

Figure 1C and D shows the corresponding elemental composition of QDs obtained by X-ray photoelectron spectroscopy taken for Cd 3d and Zn 2p regions. The two strong peaks in Figure 1C at 411.7 eV (Cd $3d_{5/2}$) and 405.0 eV (Cd $3d_{3/2}$) are associated with the Cd (3d) transitions in CdS. The spin-orbit components (Cd $3d_{5/2}$ and Cd $3d_{3/2}$) are separated by a binding energy interval of ~6.7 eV.[29,32,33] In Figure 1D, the peaks at 1,022.0 eV and 1,044.9 eV correspond to the Zn $2p_{3/2}$ and Zn $2p_{1/2}$ levels, respectively, which are generally assigned to Zn–S bonding in ZnS. The difference between the binding energies of Zn $2p_{1/2}$ and Zn $2p_{3/2}$ is 23.0 eV, which is in agreement with literature.[33–35] The S $2p_{3/2}$ peaks (Figure 4) were found at 161.3 eV (CdS) and 161.4 eV (ZnS), which can be assigned to oxidation state of sulfur (-2) in metal sulfides.[32–35]

ZP analysis of the nanoconjugates in colloidal media showed practically neutral charges at pH=6.0, due to the deprotonation of amine groups of CHI ligands near its pKa (~6.5). The DLS measurements showed hydrodynamic diameter (HD) values of 13.7 nm and 22.8 nm for CdS (Figure 1E) and ZnS (Figure 1F), respectively, which clearly indicated a higher volume of solvation for the ZnS nanoconjugates that is assigned to the higher stability of the Cd^{2+} chelate complex formed predominantly with the amine groups of CHI (Equation 2) compared to Zn^{2+},[36] which probably caused the contraction of the polymeric organic shell around the QD inorganic core, measured by DLS.

$$M^{2+}_{(aq)} + L_{(aq)} \rightarrow [ML]^{2+}_{(aq)};\ [ML]^{2+} + L_{(aq)} \rightarrow [ML_2]^{2+}_{(aq)};\ \ldots.\ [ML_{n-1}]^{2+} + L_{(aq)} \rightarrow [ML_n]^{2+} \quad (2)$$

In previous studies,[15,37,38] our research group synthesized and characterized the stabilization of QDs by CHI and its derivatives, which is essentially due to the interactions of the chemical functional groups of the polysaccharide

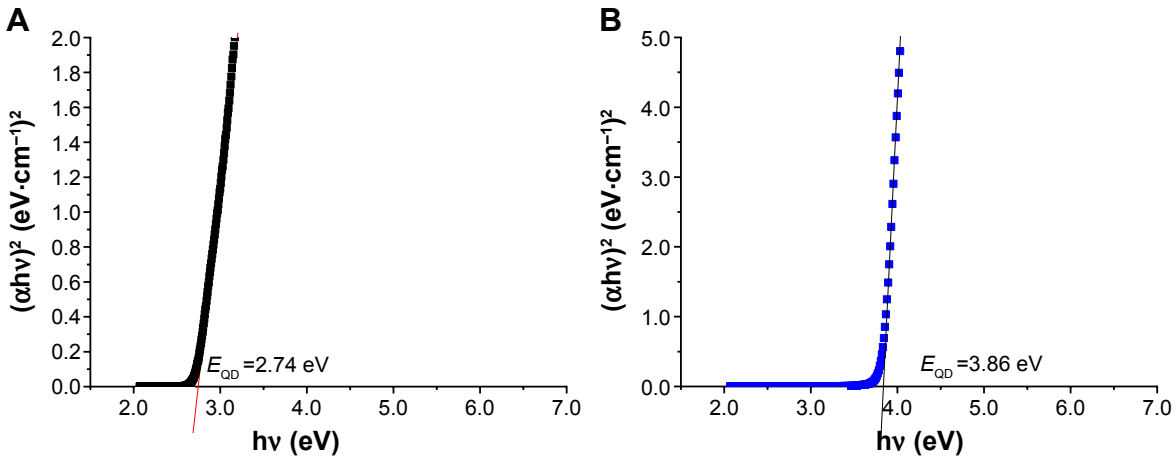

Figure 2 Optical band gap using "Tauc" relation: (**A**) CdS and (**B**) ZnS.
Abbreviations: E_{QD}, band gap energy; eV, electron-volt; α, absorption coefficient; h, Planck's constant; υ, frequency of the radiation.

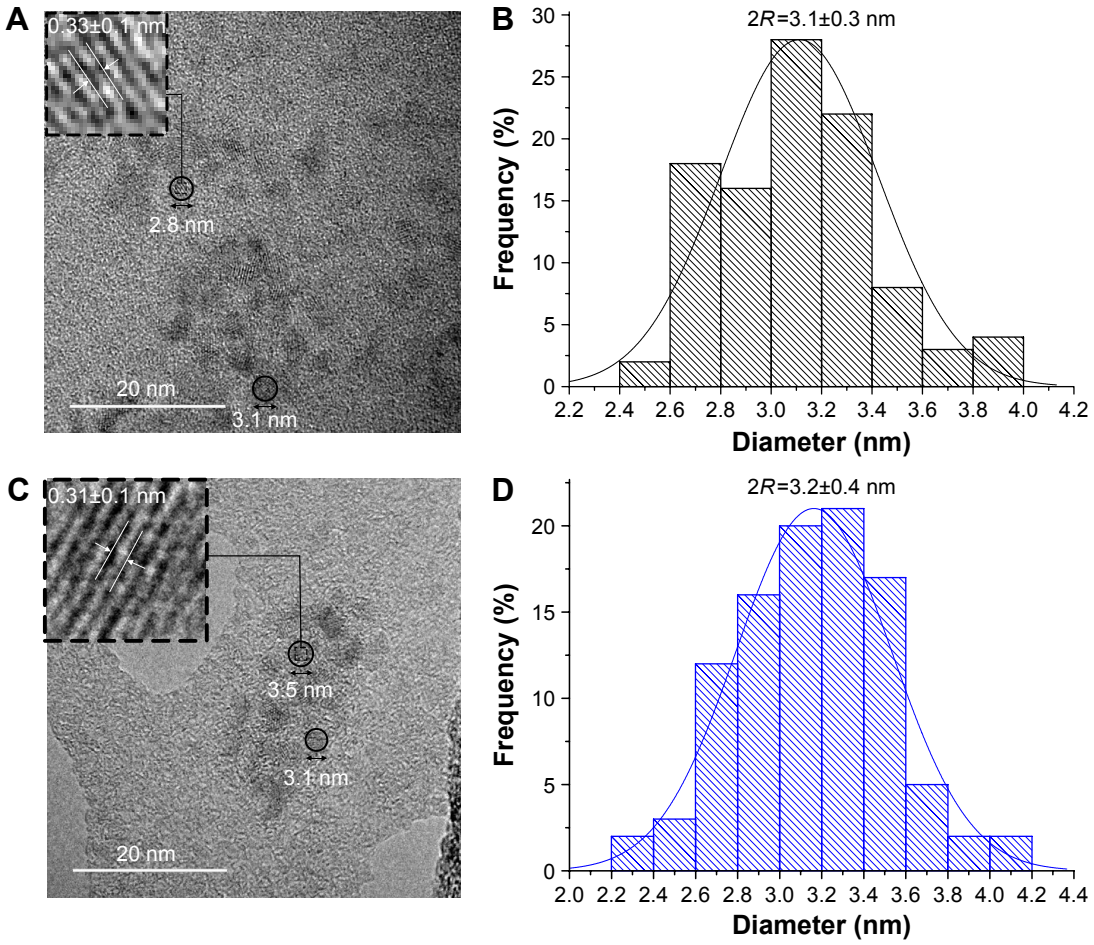

Figure 3 TEM image, (**A**) CdS and (**C**) ZnS, and histogram of nanoparticle size distribution, (**B**) CdS and (**D**) ZnS.
Note: Insets: nanocrystal plane spacing.
Abbreviations: TEM, transmission electron microscopy; 2*R*, nanoparticle diameter; nm, nanometer.

polymer chains, ie, predominantly amines (NH_2) and hydroxyls (OH), with the metallic cations (Cd^{2+} or Zn^{2+}) present at the QD surfaces. Therefore, CHI and its derivatives behave simultaneously as chemical capping ligands and biocompatible layers, comparable to other polymeric alternatives widely used for biomedical applications of particulate conjugates such as polyethylene glycol and polyvinyl alcohol.[19,39]

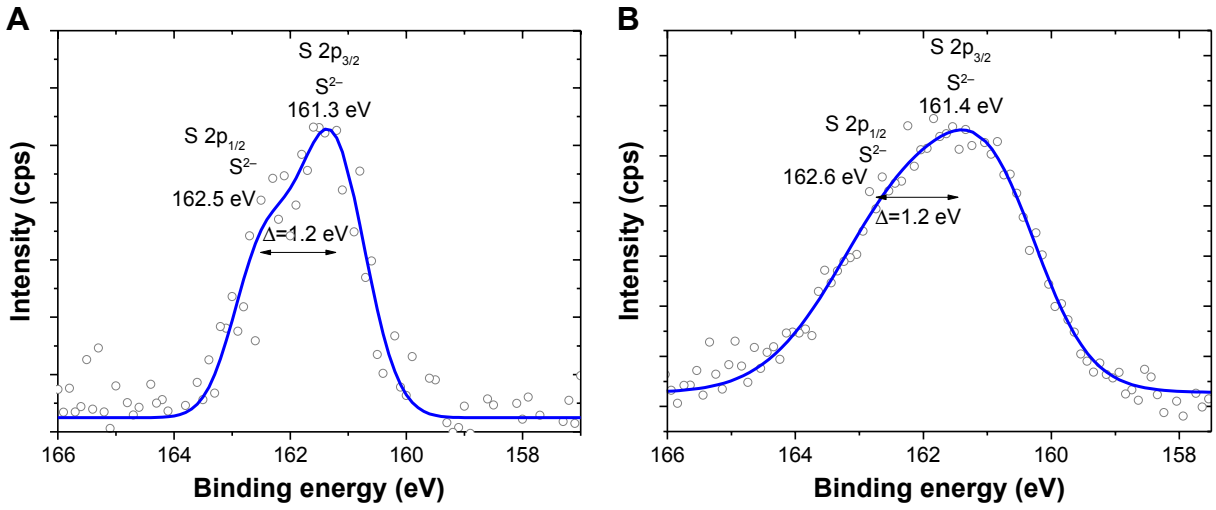

Figure 4 XPS spectra of CdS and ZnS nanoconjugates: S 2p region for CdS (**A**) and ZnS (**B**).
Abbreviations: XPS, X-ray photoelectron spectroscopy; Δ, spin orbit separation; cps, counts per second; eV, electron-volt.

Regarding the toxicity analysis of CdS and ZnS QDs biofunctionalized with CHI, an important set of physicochemical properties has been identified that need to be addressed in toxicological studies of engineered functional nanomaterials. They include size and size distribution, state of dispersion, HD, surface charge, chemical composition, surface area, and surface chemistry. These physicochemical properties of nanoparticle colloidal dispersions can have a strong effect on the way in which living organisms respond upon exposure and therefore need to be properly characterized and understood.[40] Thus, these key parameters were investigated in this study, and the results were interpreted regarding their effect in the cytotoxicity responses toward the CdS and ZnS nanoconjugates. The core sizes of the CdS and ZnS QDs are similar (~3.0 nm, within 10% variation) for both systems, but the HD values are very distinct and, therefore, they must be considered when analyzing the cytotoxicity of these nanostructures. It has been proposed in the literature that the reduction in the nanoparticle size is an important factor for increasing its toxicity.[9] A key aspect of nanoparticle toxicity is the size-dependent endocytosis and intracellular routing because nanoscale particles are able to reach organelles that are inaccessible to metal ions, which may result in unique patterns of cytotoxicity.[5] This aspect cannot be separated from the others, but it is one of the most relevant physiochemical features to be considered in the overall toxicity response of cells. In addition, surface charge can play an important role on the toxicity of QD-based conjugates. In this study, ZP measurements for both systems with CdS and ZnS QDs showed equally neutral values (~0 mV). Thus, considering that most of the physicochemical properties, ie, core size of QDs, ZP values, and surface chemistry (CHI), are similar for both conjugates, the differences to be taken into account associated with their potential toxicity are the chemical composition of semiconductor core, CdS or ZnS, and the average HD values, 13.7 nm and 22.8 nm, respectively. In this sense, based on these two aspects, CdS nanoconjugates are likely to present much more toxicity than ZnS conjugates, as they are made of highly toxic inorganic Cd-based core combined with a smaller HD dimension compared to ZnS QDs with a larger HD size. Reports in the literature[5,7] indicated that the smaller the QD, the more tendency to undergo endocytosis and cause harmful cellular effects. To verify these hypotheses, a set of biological cell viability assays and cellular uptake in vitro tests were designed and performed in this study. In addition, in vivo assays were performed using BALB/c mice, and the results are presented in the following sections. However, it is important to highlight that despite its undisputable relevance, it is not conceivable to perform all biological assays related to the theme of nanotoxicity and the in-depth investigation of the mechanisms involved in vitro and in vivo is beyond the focus of this study.

Biological characterization of QD–CHI nanoconjugates

Biological characterization by MTT cell viability assay

In the present study, key processing variables were selected to investigate the cytotoxicity of the nanoconjugates made of QDs (core) and aminopolysaccharides (CHI – shell), which were: a) inorganic binary semiconductor CdS or ZnS; b) concentration; c) time of exposure; and d) three types of cultured cells: kidney cell line of a human embryonic culture (HEK293T), human sarcoma cell line culture (SAOS), and non-Hodgkin's B-cell lymphoma/ATCC-CRL-2631 (Toledo).

Here, the cytotoxicity of core–shell MS-QD/CHI (M = Cd or Zn) nanoconjugates was assessed using the enzyme-based MTT assay, which is used in >50% of the published articles investigating cytotoxicity of Cd-containing QDs accordingly to the recent literature survey.[9]

The MTT results of CdS QD nanoconjugates are displayed in Figure 5. A general trend was observed regarding the cytotoxicity of CdS nanoconjugates for the three cell types. At short incubation period (72 hours, 3 days) and low concentration (1%), only minor adverse response on cell viability (ie, >80% viability) was detected. However, at longer incubation period (168 hours, 7 days) and higher concentration of CdS conjugates (10%), a significant reduction in the cell viability responses was observed for all systems, with a drastic decrease of >50% toward HEK293T and SAOS cell types and moderate decrease of ~20% for Toledo cell type. It is worth emphasizing the relative high resistance of Toledo cell toward the CdS nanoconjugates, where minor cytotoxicity was verified even at the most harsh testing conditions (ie, 7 days, 10% concentration).

Analogously, the MTT results of ZnS QD conjugates are presented in Figure 5. Obviously, no significant toxic effect of ZnS-based nanoconjugates at the same conditions tested for the CdS QD systems was observed. The cell viability responses of HEK293T and SAOS types toward ZnS conjugates were predominantly >80% for all concentrations (1%, 5%, and 10%) and exposure time periods (1 day, 5 days, and 7 days). In addition, the cell viability results of Toledo type were statistically similar to control groups (ie, 100%). The overall comparison of the MTT results of CdS and ZnS nanoconjugates is summarized in Figure 6, with the most and least sensitive cell types (ie, HEK293T and Toledo, respectively), at the lowest and higher concentrations (1% and

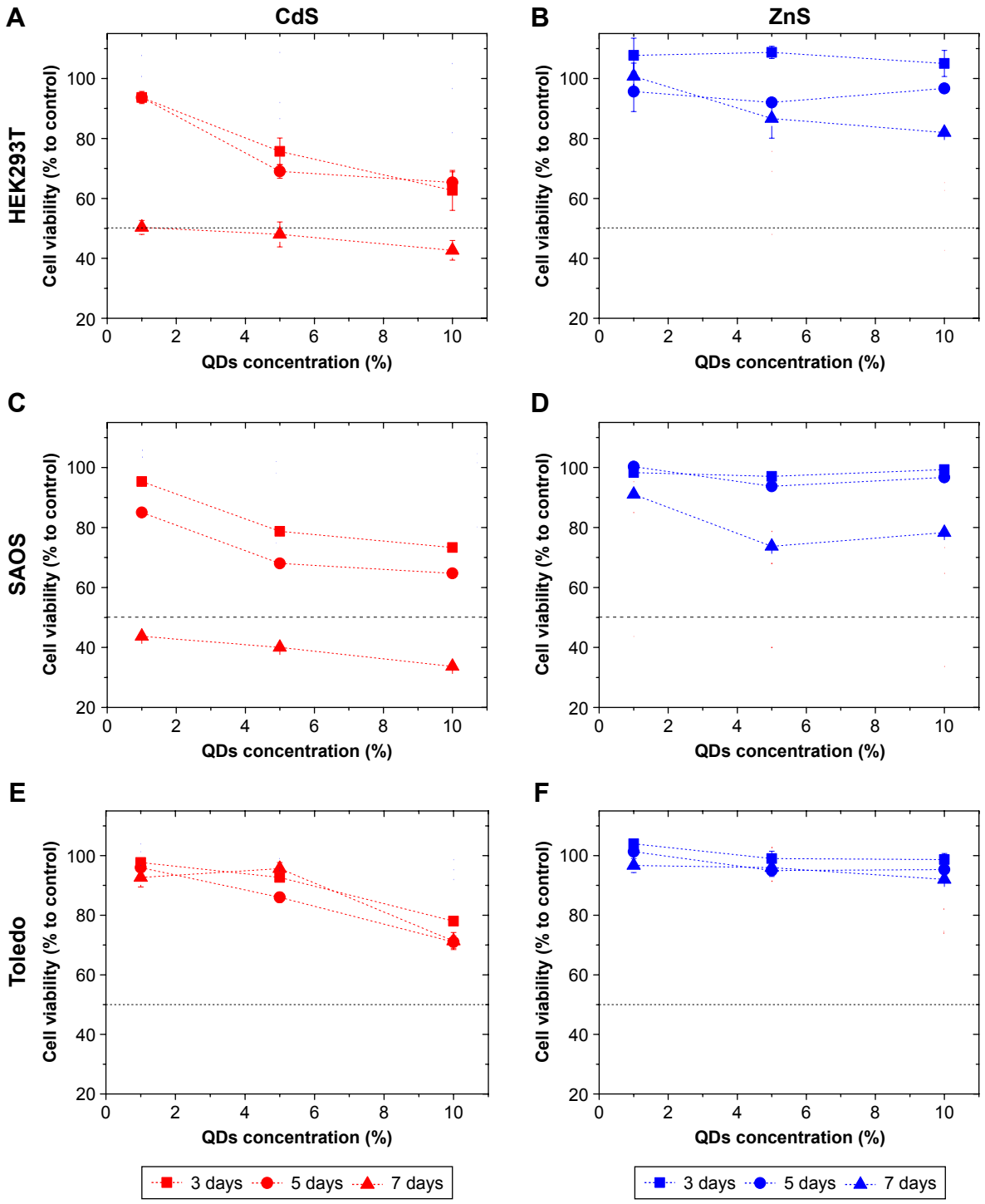

Figure 5 Cell viability response of HEK293T, SAOS, and Toledo cell cultures using the MTT assay for CdS, (**A**), (**C**), and (**E**), respectively; and ZnS, (**B**), (**D**), and (**F**), respectively.

Abbreviations: HEK293T, human embryonic cell line; SAOS, human sarcoma cell line; MTT, 3-(4,5-dimethylthiazol-2-yl)-2,5-diphenyltetrazolium bromide; QDs, quantum dots.

10%), after the longest incubation period (7 days). In addition, no alterations in the morphological and shape features of the HEK293T and Toledo cells were observed when tested with ZnS nanoconjugates, presenting 100% cell confluence (Figure 6C and E). However, CdS nanoconjugates caused significant reduction of cell confluence, predominantly of the HEK293T cells even at the lowest concentration (1%; Figure 6D).

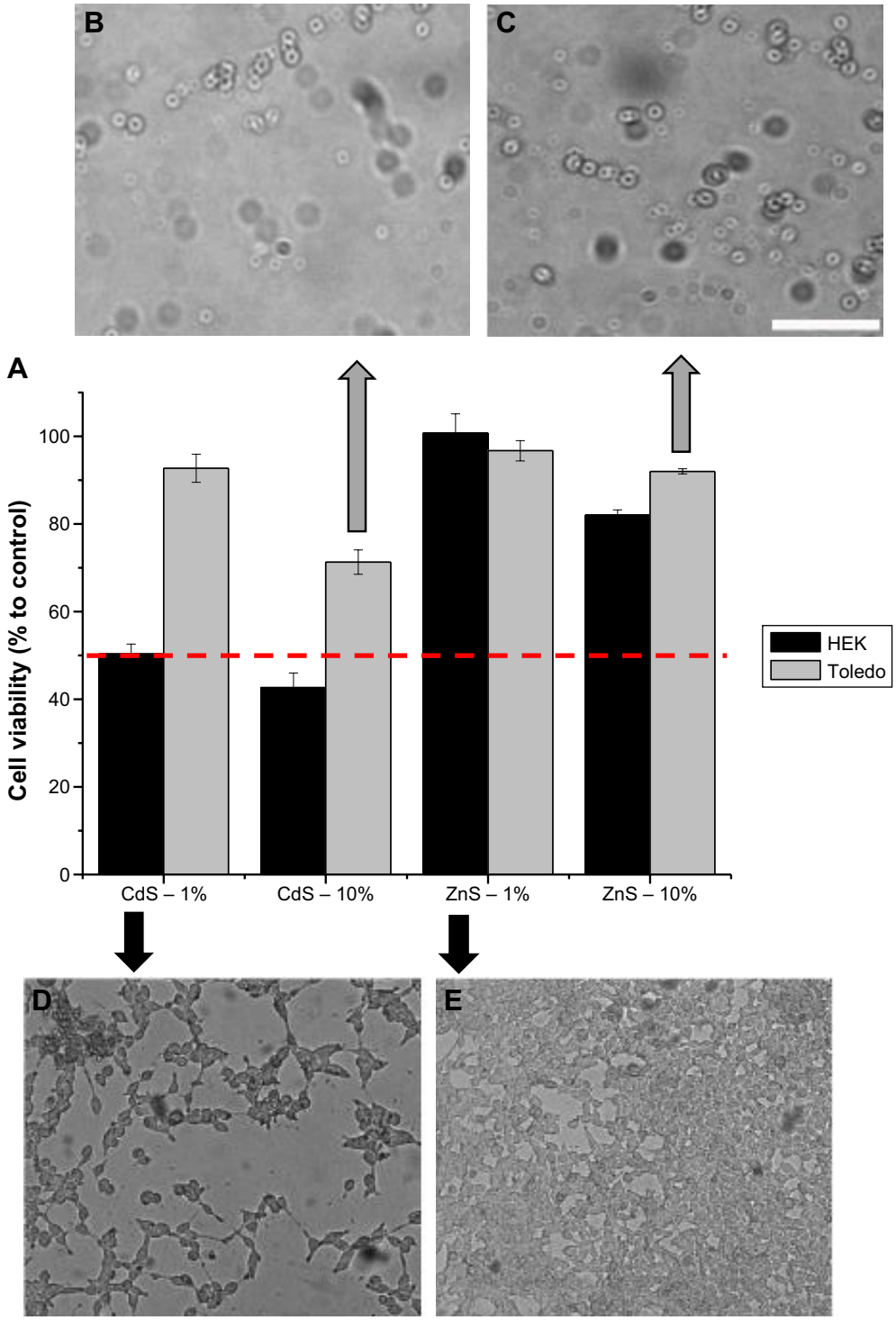

Figure 6 Comparison of the MTT results of CdS and ZnS.
Notes: HEK293T and Toledo cell viability responses by MTT assay after 7 days of incubation in direct contact with the CdS and ZnS nanoconjugate samples (**A**); Red line indicates the separation between toxic (less than 50%) and non toxic (more than 50%) response. Morphology of Toledo cells in CdS, 10% (**B**), and ZnS, 10% (**C**), samples. Morphology of HEK293T cells in CdS, 1% (**D**), and ZnS, 1% (**E**), samples (scale bar =100 μm).
Abbreviations: HEK293T and HEK, human embryonic cell lines; MTT, 3-(4,5-dimethylthiazol-2-yl)-2,5-diphenyltetrazolium bromide; μm, micrometer.

Rationale

Based on the MTT analyses performed in this research, the CdS QD nanoconjugates showed increased toxicity at higher concentrations and longer incubation time. Despite the common strategy broadly reported in the literature of using biocompatible capping ligands for synthesizing Cd-containing QDs,[5] in this study, it is demonstrated that the CdS QDs functionalized with CHI, a natural

aminopolysaccharide, which is known as biocompatible capping polymer for nanomaterials, have not entirely prevented the cytotoxic behavior at long exposure periods and high concentrations for HEK293T and SAOS cell types. These results can be interpreted considering that Cd^{2+} is highly toxic and several in vitro studies have demonstrated that Cd-containing QDs showed harmful effects on the cells when the nanoparticles are degraded in the biological environment. The Cd-based nanoparticle-induced cell cytotoxicity is associated with mechanisms involving both the release of Cd^{2+} and generation of reactive oxygen species accompanied by lysosomal enlargement and intracellular redistribution, leading to apoptosis and cell death.[41–43] Hence, the reduction in cell viability responses of HEK293T and SAOS at longer exposure periods and higher concentrations of CdS nanoconjugates can be attributed to the possible release of Cd^{2+} ions causing cell death. On the other hand, the surprising results in this study indicating a high resistance of Toledo cell type toward the CdS nanoconjugates were completely distinct from the results of HEK293T and SAOS cells, where no significant cytotoxicity was verified even at severe conditions tested (ie, 7 days, 10% concentration).

Here, we attempted to suggest plausible explanations to this unusual resistance of Toledo cell with CdS nanoconjugates that can be related to the combination of two predominant aspects: a) it is an immortalized cancerous cell line from B-cell lymphoma and b) B-cell has a key function in the humoral immunity component of the adaptive immune system by secreting antibodies. Thus, Toledo exceptional resistance toward toxic microenvironments is accounted to the fact that it is derived from natural defense of immune system of mammals associated with the highly resistant and proliferative features common to cancer cells. Each cell type can express varying membrane receptors and can utilize different internalization pathways, and the behavior of nanoparticles in endolysosomal vesicles remains not clearly understood, with some evidences suggesting that the protease enzymes inside endolysosomal vesicles cleave nanoparticle ligands. In addition, studies in the literature reported that the endocytic pathways of defense cells (eg, macrophages and B-cells) are distinct as the endolysosomal vesicles tend to accumulate the toxic species for much longer periods without releasing them into the cytosol. If toxic cores of QDs (eg, Cd^{2+}) are released into the cytosol, they can elicit biological responses by disrupting mitochondrial function, producing reactive oxygen species and activating the oxidative stress-mediated signaling cascade, leading to apoptosis and cell death.[44–46] Moreover, B-cell lymphoma overexpresses metallothionein (MT; low molecular weight 6–7 kDa), a metal-binding protein of animal kingdom that is induced at the transcriptional level by cadmium and tightly binds metal ions. Increased expression levels of MT protein have generally been related to cancer cell survival and resistance to various proapoptotic regimes, including chemotherapy and radiation.[47–50] Hence, our cell viability results support the hypothesis that Toledo cells have more complex endocytosis pathways and intrinsic intracellular features (eg, higher content of MT protein for binding heavy metal ions) than the other cell types (ie, HEK293T and SAOS), which may have minimized the harmful effects of highly toxic Cd^{2+} eventually released by the nanoconjugates, rendering them more resistance to cytotoxic compounds. Such observations, endorsed by the results found in the literature,[9] have caused serious concerns in recent years about whether or not to pursue the translation of Cd-containing QDs into clinical research and applications, because no definitive "risk-free" solution has been developed yet.

In this scenario, zinc-based QDs have been suggested as a promising alternative of fluorescent nanomaterials to substitute toxic Cd^{2+} of the inorganic core for biomedical applications, because they are one of the most abundant metallic ions in human body, second only to iron. The schematic representations of uptake and endocytosis pathway for CdS and ZnS nanoconjugates are depicted in Figure 7A and B, respectively. Obviously, this is a simplified scheme based on the cell viability responses and endocytosis toward the QD nanoconjugates. Additional bioassays can be designed and performed for signaling apoptosis and cell death mechanisms involved in nanotoxicity using specific biomarkers (eg, annexin/propidium iodide) but not directly accessing the real-time concentration of metal cation species "free" at the micro–nanoenvironment. Multiple cell–nanoparticle interactions occur at these complex and dynamic biointerfaces, which have been the subject of intense research reported in the literature[43–46,51,52] and is beyond the focus of this study. Nonetheless, according to the most recent comprehensive review so far addressing the toxicity of QDs published by Oh et al,[9] >50% of articles evaluated the toxicity of Cd-containing QDs using MTT cell viability assay. Moreover, MTT test is globally accepted by regulatory agencies (such as US Food and Drug Administration) as the standard protocol method for assessing the toxic effect of biomaterials and medical devices (ISO 10993-5:2009 – Biological evaluation of medical devices: tests for in vitro cytotoxicity).

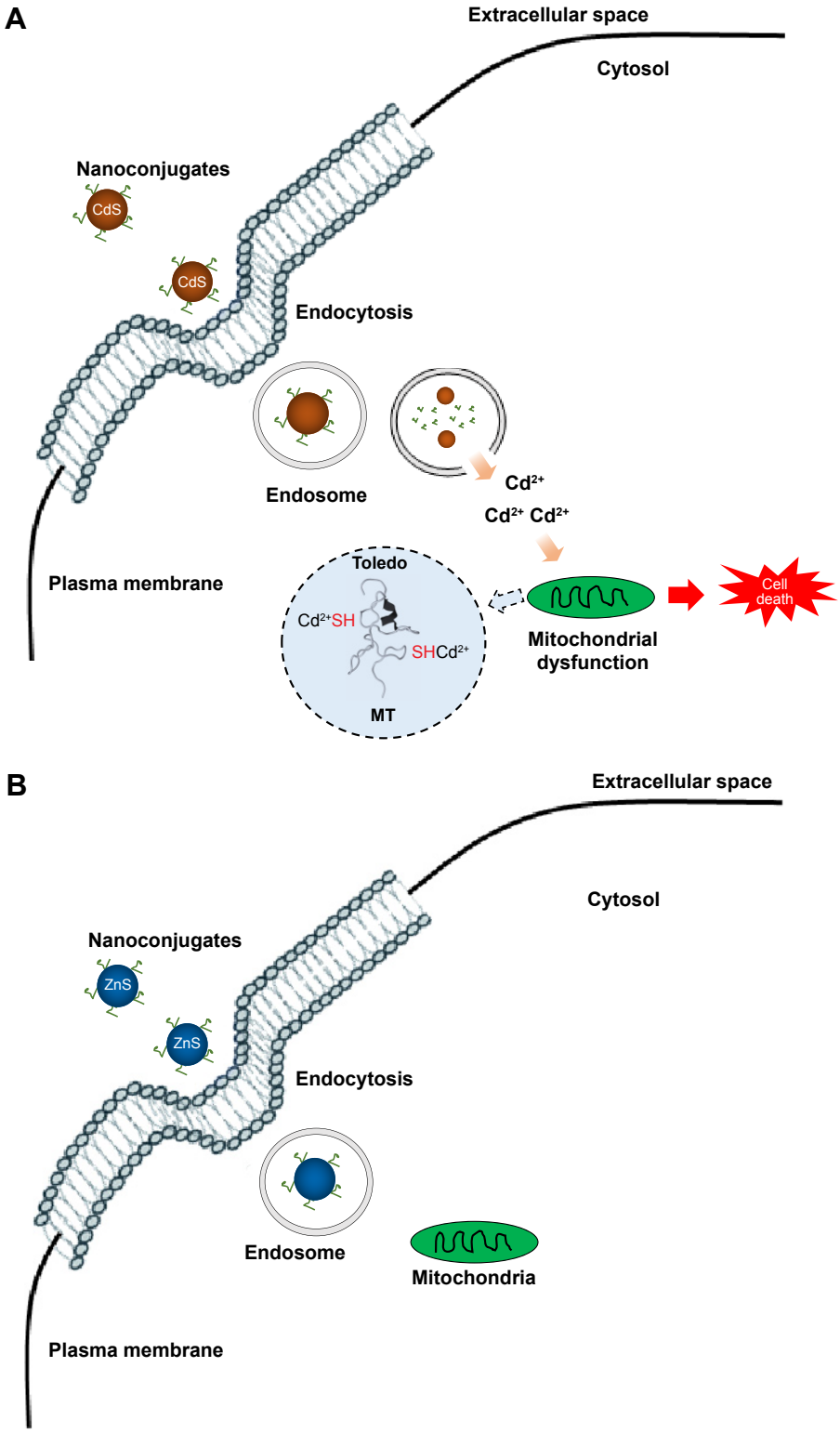

Figure 7 Schematic representation of cellular uptake and endocytosis pathway of CdS (**A**) and ZnS (**B**) conjugates.

Therefore, in this study, the MTT results of cell viability of ZnS–CHI nanoconjugates under all incubation periods, all concentrations, and the three cell types evaluated in vitro validated the hypothesis that the intrinsic nontoxicity of ZnS QD core combined with a biocompatible organic shell can be considered a "safe strategy" to produce fluorescent nanoprobes for biomedical applications.

On the contrary, the results of cell viability of CdS–CHI nanoconjugates showed strong evidences that this system cannot be considered "safe" as the toxicity was very much dependent on the time of incubation, concentration, and cell type, which can pose great risk for biological, pharmaceutical, and clinical applications.

Biological characterization by Live/Dead™ cell toxicity assay

In the current study, the Live/Dead™ assay was used as a complementary test to corroborate the toxicity results of cell viability assay by MTT. To avoid redundancy, the Live/Dead™ test was performed only with SAOS cells, which presented intermediary cell viability response between HEK293T and Toledo regarding the cytotoxicity toward CdS nanoconjugates. The relative toxicity analysis was performed by cell counting using image processing software (ImageJ, Version 1.50, freeware). Essentially, Live/Dead™ cytotoxicity method provides a cell viability assay of two color fluorescence, which is based on the simultaneous determination of live cells (stained in green) and dead cells (stained in red) by fluorescence microscopy. Hence, it can be observed in the images presented in Figure 8A that the SAOS cells in contact for 72 hours and low concentration (1%) of the ZnS or CdS nanoconjugates had fluorescence patterns similar to the control group, ie, high green fluorescence (viable cells) and no detected red fluorescence (dead cells). However, in Figure 8B, it can be noted that the SAOS cells in contact for 72 hours and higher concentration (5%) of the CdS nanoconjugates had fluorescence patterns distinct from the control group, ie, comparable green fluorescence (live cells) but relatively higher number of dead cells (red fluorescence). On the other hand, ZnS conjugates showed similar response to that of the control group. These results of the Live/Dead™ assay qualitatively and quantitatively confirmed the previous responses presented in MTT cell viability assays of CdS and ZnS nanoconjugates toward SAOS cell type, which was dependent on the inorganic core compound (CdS or ZnS) and the concentrations (ie, 1% and 5%).

In summary, the MTT cell viability results demonstrated conclusively that the CdS–CHI nanohybrids produced in this

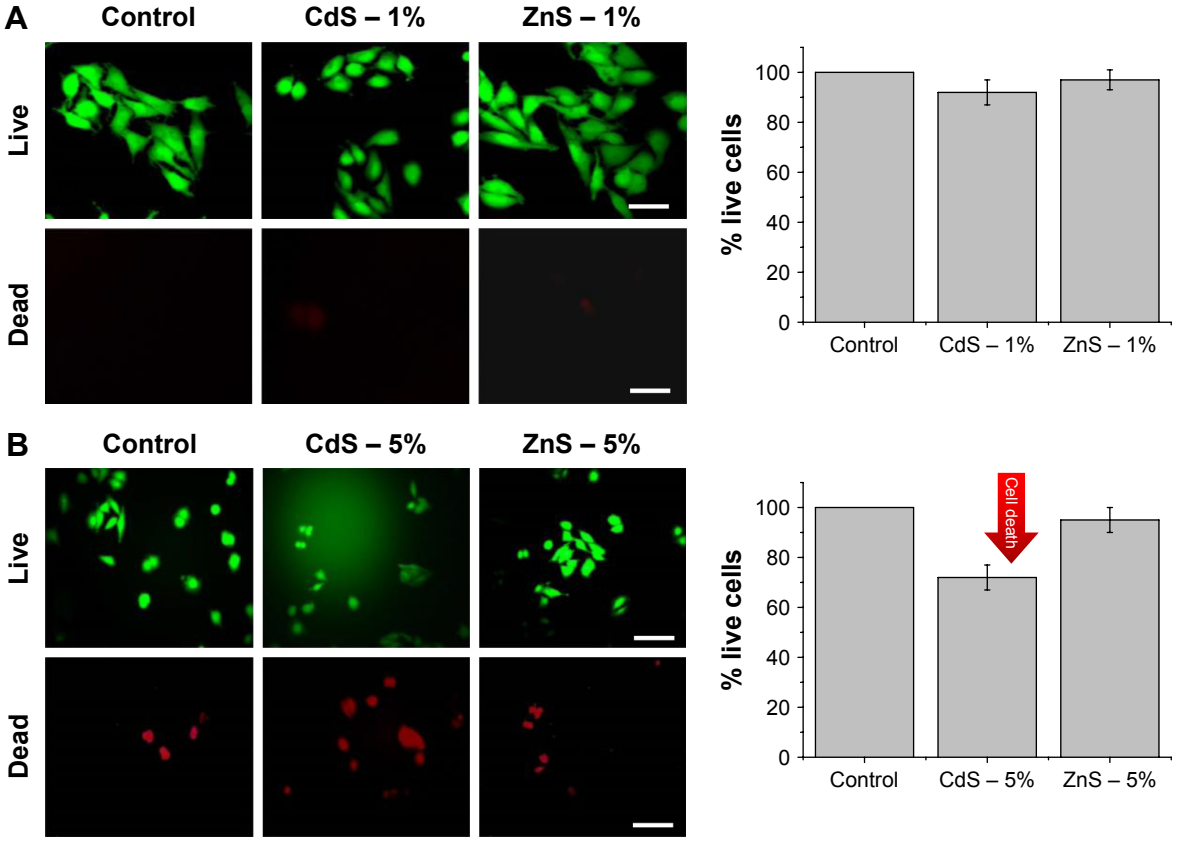

Figure 8 Live/Dead™ of SAOS cells in contact with CdS e ZnS nanoconjugates at concentration of (**A**) 1% (bar =25 μm, 400×) and (**B**) 5% (bar =50 μm, 200×) after 72 h of contact, with respective histogram of quantitative analysis of live cells.
Abbreviations: SAOS, human sarcoma cell line; μm, micrometer; ×, magnification; h, hour.

research are cell line and physicochemical dependent. More important, according to the combination of results obtained from the in vitro cytocompatibility assays, it is affirmed that the nanoconjugates made of CdS (core) and aminopolysaccharide (shell) may pose a significant and unpredictable toxic risk to cells, which should impair them to be safely used in vivo as fluorescent nanoprobes for diagnostic and bioimaging applications.

Cellular uptake of QD nanoconjugates

In order to further investigate and provide a more in-depth analysis of the toxicity responses observed for the QD nanoconjugates produced in the present study, a set of cellular uptake experiments were designed and performed. It is well known by the literature that QDs can be internalized into cells through a number of different pathways, including transfection, peptide-mediated delivery, and endocytosis. While QDs can be actively delivered into cells, a number of studies have shown that cells will uptake QDs with modified polymer coatings through endocytosis based on their surface coatings.[53–55] The first type of endocytosis discovered was clathrin-mediated endocytosis, but later several additional types of endocytosis have been identified. So far, a comprehensive understanding of the actual cellular process of the uptake and subcellular localization and distribution of QDs is very limited.[55] In the present study, examination of the uptake process of QD nanoconjugates was investigated by flow cytometry and laser scanning confocal microscopy.

Quantitative flow cytometry analysis

The internalization of QDs occurs predominantly via endocytosis pathways, which are initiated by the formation of the endosome through the invaginating plasma membrane to envelop the conjugates formed by cell receptors and nanomaterials. Subsequently, newly formed endosomes are transported through endosomal–lysosomal–autophagy pathways, as schematically depicted in Figure 7.[11] Thus, the uptake of the CdS and ZnS QD conjugates by the Toledo cells was verified by flow cytometry. Internalization of the QD-conjugated nanoparticles was evaluated in the FITC channel and merged on total Toledo population in order to verify the size and granularity of fluorescent cells. In Figure 9A, representative dot plots of flow cytometry of cells incubated with CdS and ZnS nanoconjugates showed a fluorescent positive population of 25.8% and 30.4%, respectively, while the references of cells untreated (control) and exposed only to CHI showed a very small fluorescent background of 0.3% and 1.8%, respectively. The results of quantitative fluorescence of samples are displayed in Figure 9B, where it can be clearly observed that the internalization of CdS and ZnS nanoconjugates has effectively occurred ranging from ~25% to 30%. In addition, these results are very important as they demonstrated that despite the distinct HD values of CdS and ZnS QD nanoconjugates (13.7 nm and 22.8 nm), they were similarly internalized by Toledo cells, which supports the discussion of previous section of MTT viability assay, where the toxicity response was predominantly caused by the hazardous CdS core.

Moreover, despite the presence of CdS nanoconjugates distributed uniformly in the intracellular space of Toledo cells, they must have had a superior resistance toward the toxicity of CdS because no difference in cell death was verified compared to ZnS QDs. In this sense, ZnS nanoconjugates (Figure 9B, column 2) were not cytotoxic, and the quantitative flow cytometry analysis showed relatively higher cellular uptake of these nanoconjugates compared to CdS-based samples (Figure 9B, column 1).

Endocytosis assay

In this work, Toledo, HEK293T, and SAOS cells were incubated for 1 hour with CdS and ZnS nanoconjugates at a final concentration of 500 nmol·L^{-1}. After this period of incubation, images were captured using laser confocal microscopy for the purpose of visualizing the internalization of the developed surface-biofunctionalized CdS and ZnS QDs. Figures 10 and 11 show that the CdS and ZnS nanoconjugates, respectively, were internalized by Toledo, HEK293T, and SAOS cells (control samples are presented in Figure 12). Based on these confocal microscopy images, it was verified that CdS and ZnS QD nanoconjugates penetrated through the cell membrane and, therefore, were found distributed inside the cellular cytoplasm. Cellular localization of CdS and ZnS nanoconjugates was examined using intensity fluorescence profiles obtained using image process software (ImageJ, Version 1.50). Twenty-four hours after cellular uptake of HEK293T cells, the distribution of fluorescence emission of ZnS conjugates (Figure 13A) showed noticeably preferable concentration at the boundaries (similar to the CdS nanoconjugates, not shown), where the increased intensity was due to greater density of QD nanoprobes in the region closer to the cell membrane. Conversely, more diffuse cytosolic fluorescence distribution was observed for SAOS (Figure 13B) and Toledo (Figure 13C) cell types, with no clear evidence of specific intracellular localization of the CdS and ZnS fluorophores.

Hence, it is suggested that the distinct results of intracellular membrane localization of nanoconjugates at HEK293T cells compared to SAOS and Toledo can be related to their

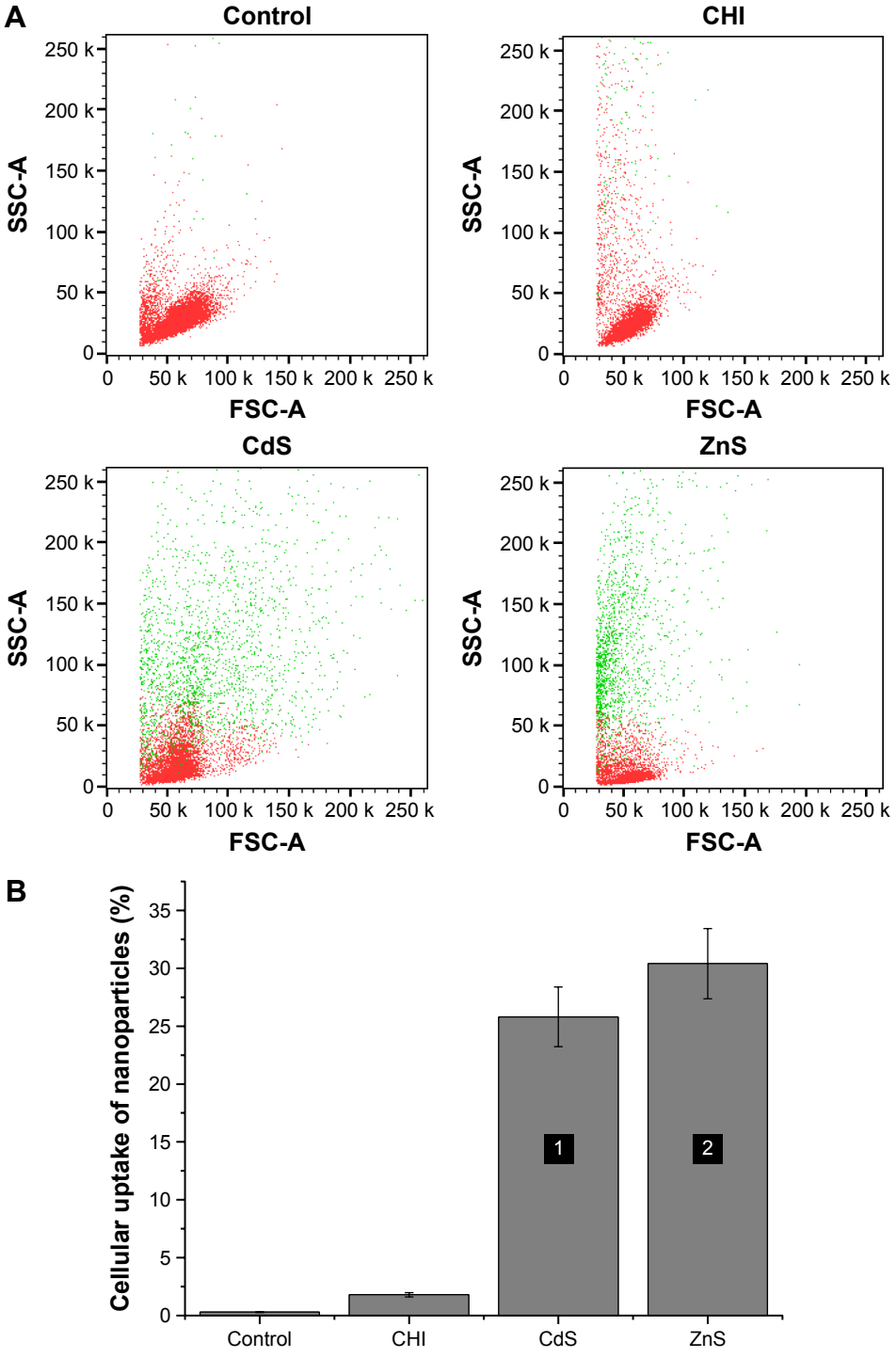

Figure 9 Quantitative flow cytometry analysis.
Notes: Dot plots (**A**) of flow cytometry of Toledo cells incubated with medium (control), with CHI, or with the QD-conjugated nanoparticles CdS and ZnS Toledo cells with fluorescence (FITC+; green); Toledo cells without fluorescence (FITC-; red). Quantitative flow cytometric analysis of the effects of using different QD-conjugated nanoparticles on the uptake response of Toledo cells (**B**). 1, CdS nanoconjugates; 2, ZnS nanoconjugates.
Abbreviations: CHI, chitosan; FSC-A, forward scatter; SSC-A, side scatter.

high permeability as they are widely used as model cell line for gene and nucleotide transfection. Thus, they have presented a different kinetics with an initial rapid nanoparticle uptake (transfected) followed by a slower diffusion of vesicles inside the cytoplasm. Nonetheless, the exact mechanism and pathways of how the nanoconjugates (ie, core–shell nanostructures) pass through the cell membranes are not known yet and are beyond the focus of this study, but it is believed that endocytosis and phagocytosis may be involved in the process.[56] Moreover, a large amount of cells were effectively

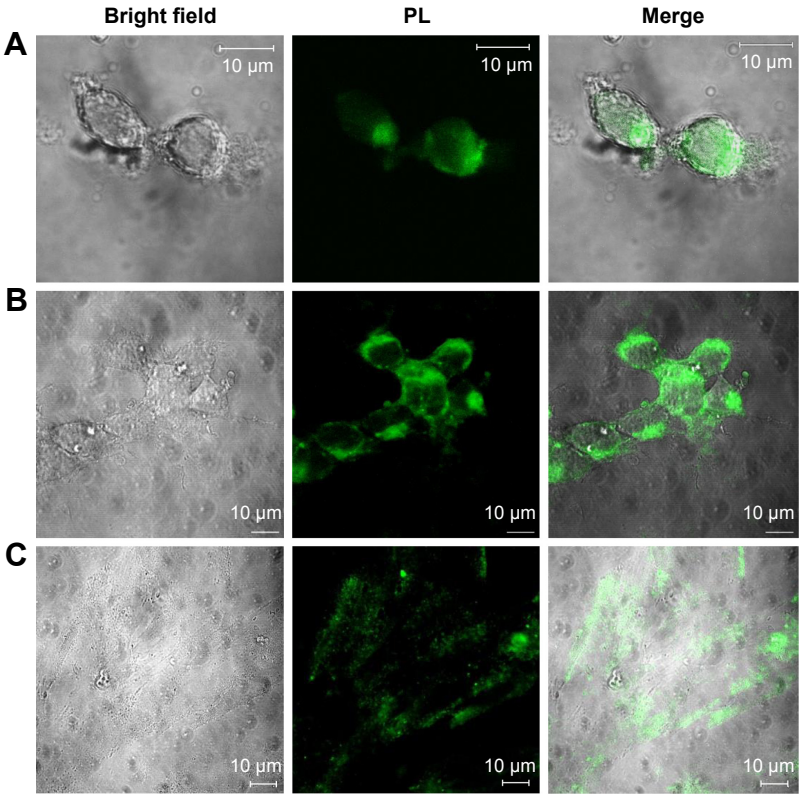

Figure 10 Confocal microscopy imaging of the cellular uptake of the CdS nanoconjugates in the Toledo (**A**), HEK293T (**B**), and SAOS (**C**) cells.
Abbreviations: HEK293T, human embryonic cell line; SAOS, human sarcoma cell line; μm, micrometer; PL, photoluminescence.

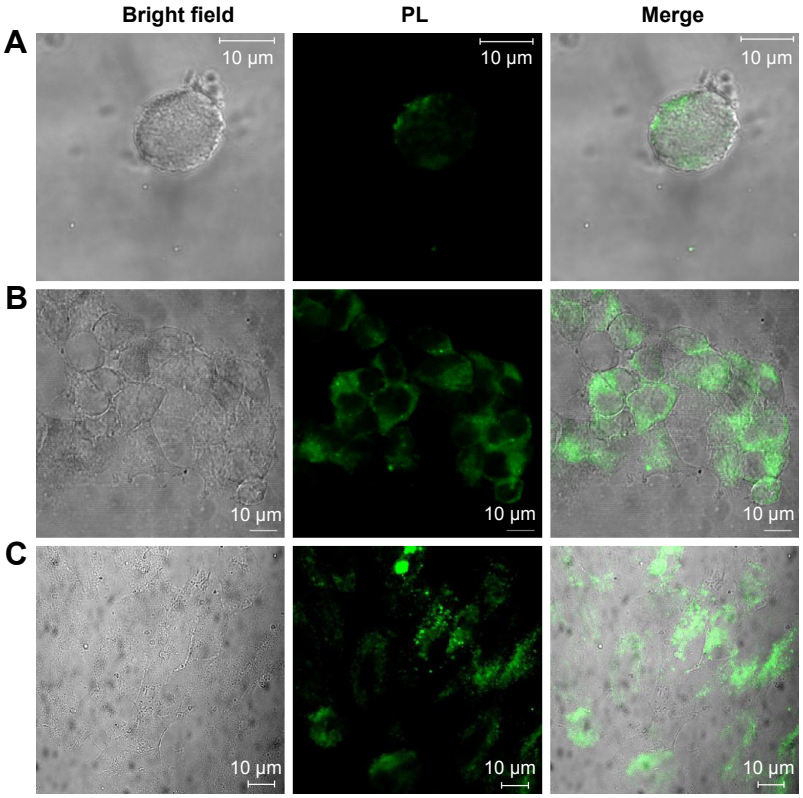

Figure 11 Confocal microscopy imaging of the cellular uptake of the ZnS nanoconjugates in the Toledo (**A**), HEK293T (**B**), and SAOS (**C**).
Abbreviations: HEK293T, human embryonic cell line; SAOS, human sarcoma cell line; μm, micrometer; PL, photoluminescence.

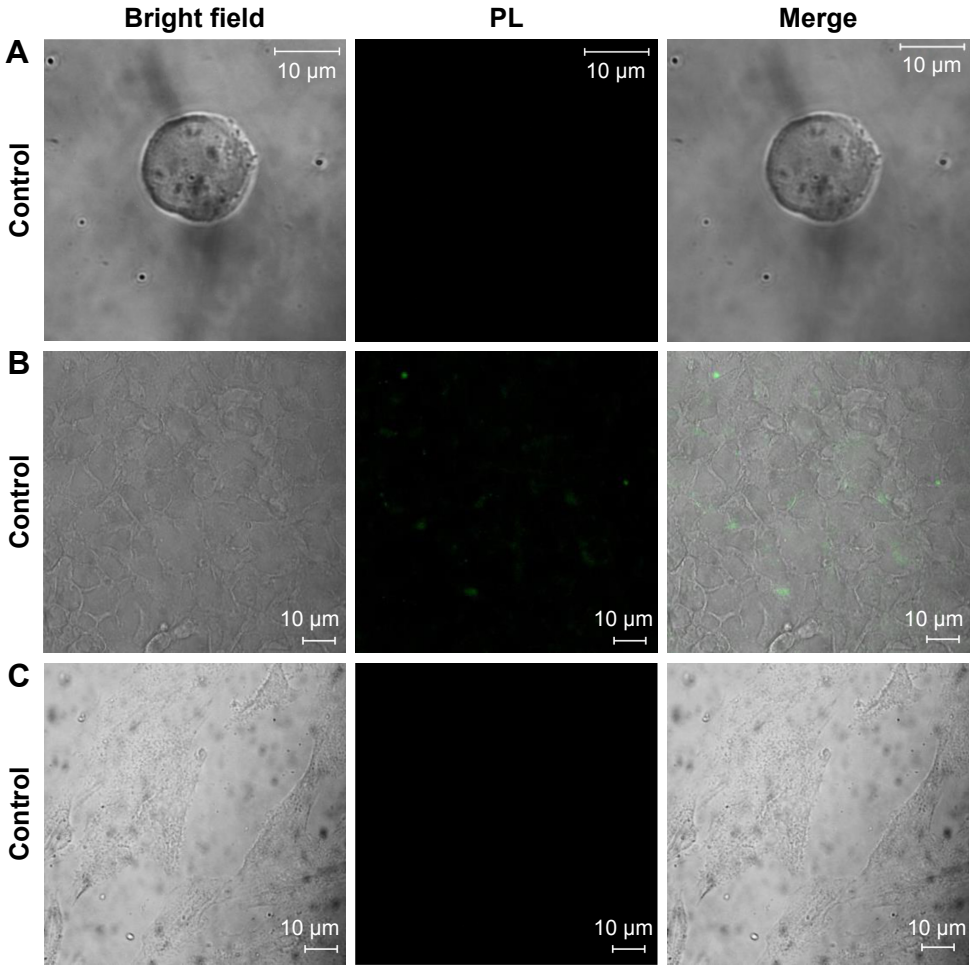

Figure 12 Confocal microscopy imaging of the Control samples for the Toledo (**A**), HEK293T (**B**) and SAOS (**C**) cells.
Abbreviations: HEK293T, human embryonic cell line; SAOS, human sarcoma cell line; PL, photoluminescence; μm, micrometer.

labeled by the fluorescent nanoconjugates, which support the hypothesis that they underwent cellular uptake through endocytic pathways and transported within the endosomal system.[57,58] Nonetheless, further investigation would be needed in future studies to enlighten the complex mechanisms of endocytosis and apoptosis involved in these CdS and ZnS nanoconjugates, which are intrinsically associated with the physicochemical and morphological properties of the nanomaterials combined with specificities of the cell lines.

In vivo studies

In order to analyze the potential toxicity of cadmium- and zinc-based QDs in an in vivo model, BALB/c mice were inoculated intravenously with both QD dispersions (CdS and ZnS) at two different concentrations.

The body weight was continuously monitored to investigate the long-term toxic effects of CdS and ZnS nanoconjugates in mice. As shown in Figure 14, no significant differences were observed in the average body weight between the treated group and control group for 30 days after intravenous injection of the QD conjugates, where a trend of gradual weight gain was observed. These in vivo results suggest that the CdS and ZnS QDs biofunctionalized with CHI shell were well tolerable in mice for the time and dose evaluated, where no detectable changes in eating, drinking, and clinical signs (eg, lethargy and weight loss) were observed. These in vivo results are apparently not coherent with the in vitro results with undisputable cytotoxicity. Therefore, in order to further investigate the distribution of QD formulations in mice, after 30 days of intravenous injection, they were euthanized and their major organs (liver, spleen, and kidney) were harvested and prepared for fluorescence microscopy imaging and histology studies. The choice to evaluate the liver, the spleen, and the kidney to monitor QD toxicity in vivo was made based on previous studies.[22,50,53,54] Our results showed that fluorescence emitted by CdS and

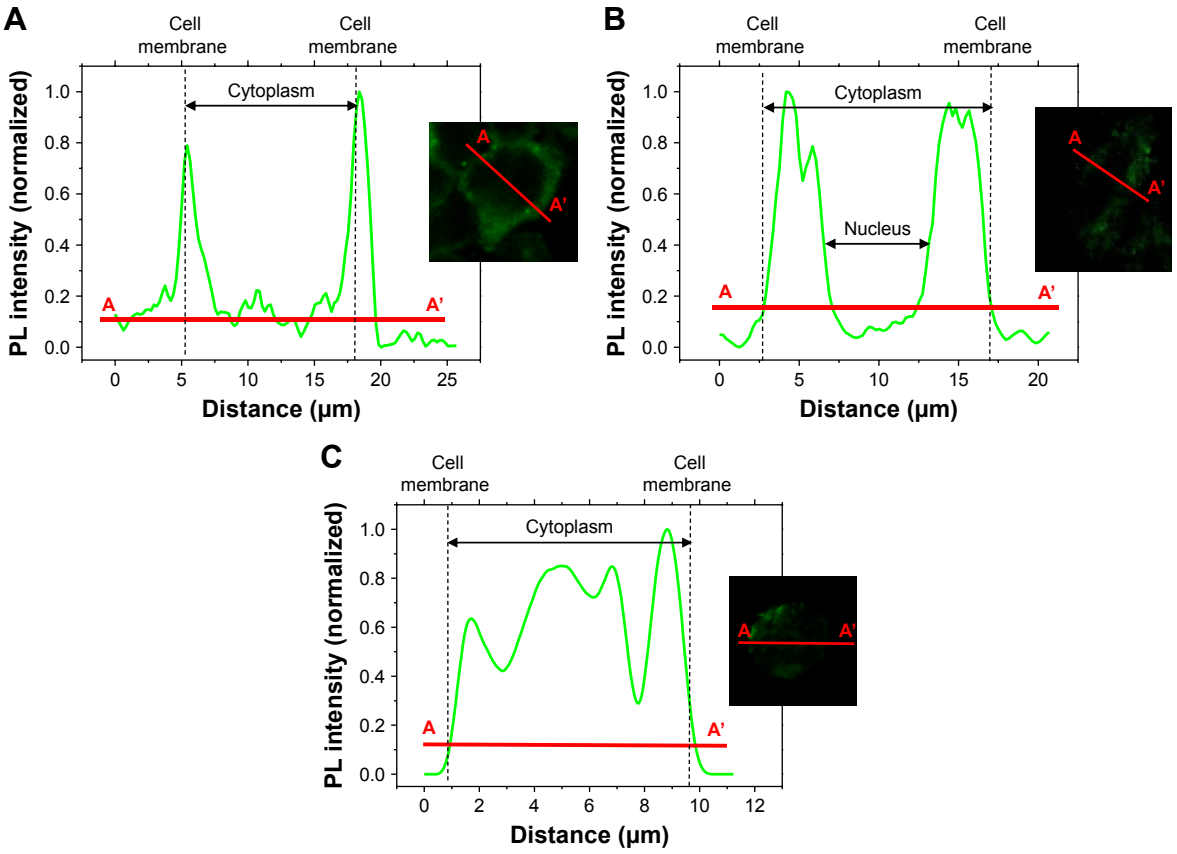

Figure 13 Intensity fluorescence profiles along A-A' line for HEK293T (**A**), SAOS (**B**) and Toledo (**C**) cell lines after 24 h of incubation with ZnS nanoconjugates.
Abbreviations: HEK293T, human embryonic cell line; SAOS, human sarcoma cell line; h, hour; A-A', cross section; PL, photoluminescence; μm, micrometer.

ZnS QDs was observed in the liver specimens after 30 days of injection (Figure 15). As a reference, the control sample indicated minor fluorescence that was subtracted from QD emission intensity (Figure 16). These results are endorsed by the literature, where it has been widely reported that the liver is the primary site for acute damage from Cd^{2+} (release of Cd^{2+} ions by CdS QDs) and a major accumulation site for nanoparticles.[22] Liver is one of the target organs after postintravenous injection of QDs, because as a reticuloendothelial system, it can clear the circulating nanoparticles from the intravenous exposure route by resident phagocytes.[50,53,54] These results manifest that the majority of CdS QD nanoconjugates were taken up by the liver and remained practically intact in this organ with sustainable fluorescence emission detected.

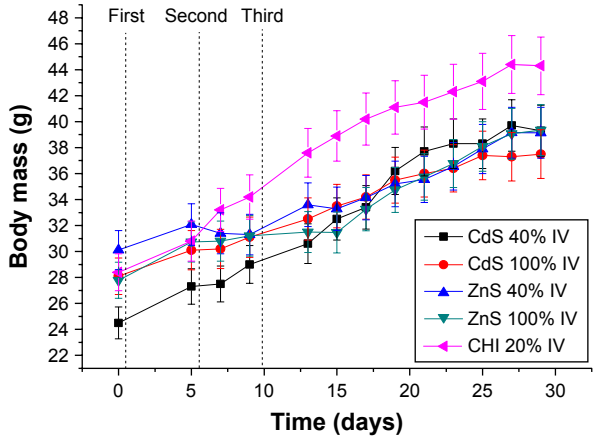

Figure 14 Weight measurements of BALB/c mice after intravenous injection of CdS and ZnS nanoconjugates and control sample (CHI 20% IV).
Abbreviations: CHI, chitosan; IV, intravenously; g, gram.

The histological assessment of liver, spleen, and kidney was conducted to determine if cadmium and zinc ions could have caused tissue damage, such as inflammation and signs of degeneration or necrosis. Overall, no significant lesions were observed in the liver, spleen, and kidney. A few hepatocytes located in zone 3 of the liver of one mouse from group 1 (inoculated with 1.0 $\mu mol \cdot L^{-1}$ CdS QDs) presented signs of degeneration, characterized by the presence of vesicles in the cytoplasm (macrovesicular steatosis; data not shown). Neither clinical alterations nor tissue damage was observed in the liver, spleen, and kidney through histological analysis. Therefore, even at high doses, either CdS or ZnS QDs did not cause significant toxicity in BALB/c mice under the experimental conditions of the present study.

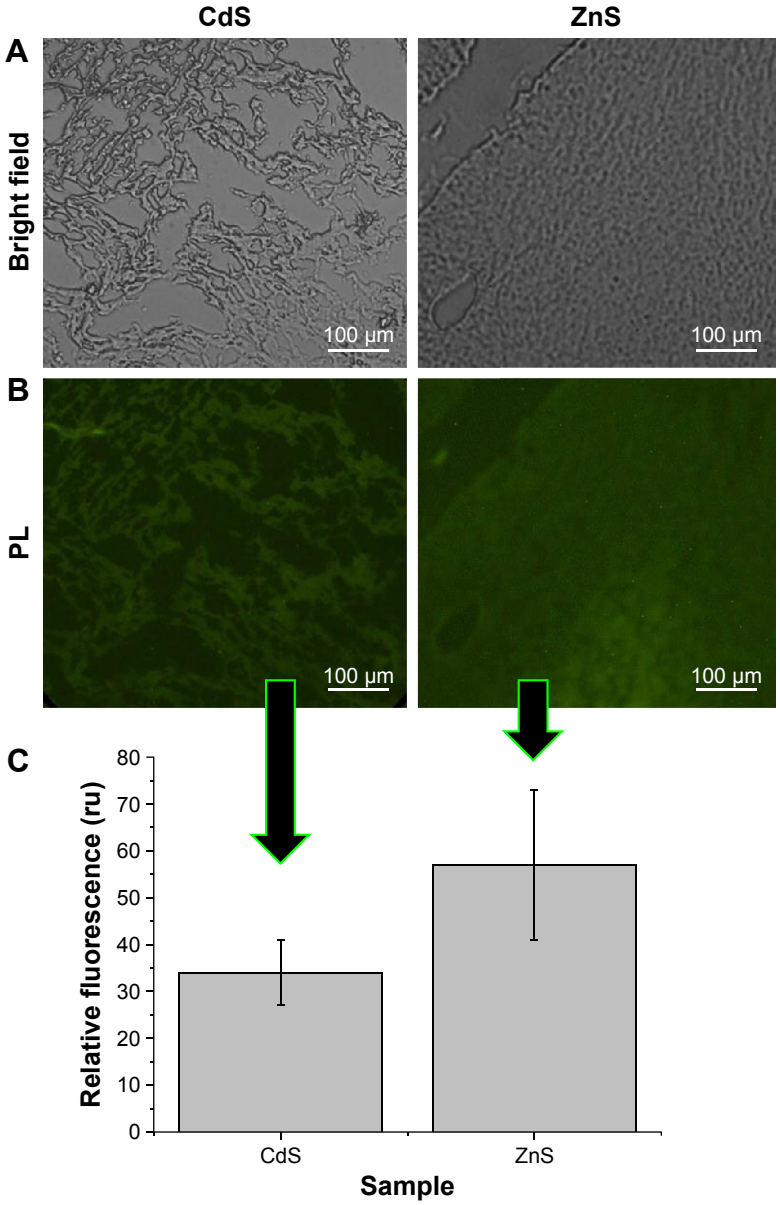

Figure 15 Fluorescence microscopy results of liver tissues.
Notes: Typical images of liver of the mice injected with pure CdS and ZnS colloidal dispersions (100% IV): optical bright field (**A**) and fluorescence emission (**B**). Histogram of relative fluorescence of tissue (control subtracted; **C**).
Abbreviations: IV, intravenously; PL, photoluminescence; ru, relative units.

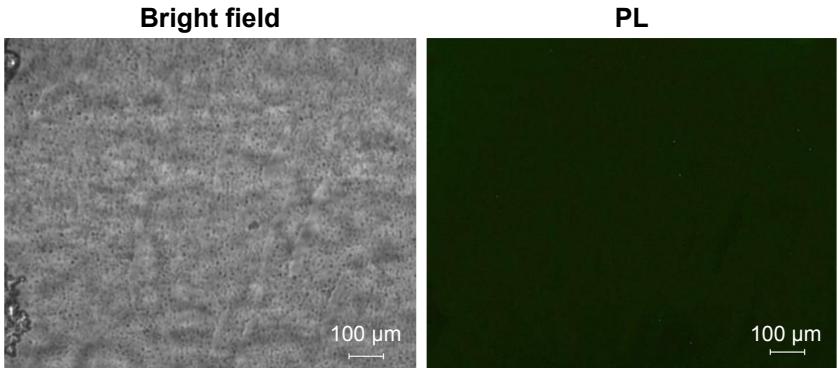

Figure 16 Typical images of liver of the mice injected with 20% CHI IV (control): optical bright field (left) and fluorescence emission (right).
Abbreviations: CHI, chitosan; IV, intravenously; PL, photoluminescence; µm, micrometer.

Conclusion

In this study, it is demonstrated that Cd-containing QDs with surface biofunctionalization of CHI as a biocompatible shell-capping ligand presented in vitro cytotoxicity responses remarkably depending on the cell type, concentration, and time period of exposure to the colloidal nanoconjugates. The concentration of CdS nanoconjugate was the predominant factor determining its toxicity followed by the time of incubation tested with HEK293T and SAOS cells. Nonetheless, the analogous systems based on ZnS–CHI nanoconjugates presented noncytotoxic responses with all the parameters investigated. These results were assigned to the potential intracellular release of Cd^{2+} after the nanoparticle uptake, leading to cell death, which were cell-type specific, where lymphoma cells showed suitable cell viability responses even at severe conditions with CdS conjugates. Unexpectedly, no decisive evidence of nanotoxicity of CdS and ZnS conjugates was observed in vivo using intravenous injections in BALB/c mice for 30 days, with minor localized fluorescence detected in liver tissue specimens. Moreover, the biological response in vitro of ZnS nanoconjugates proved that the "safe by design" concept used in this research, combining a nontoxic inorganic QD core made of ZnS with a biocompatible CHI shell layer, could benefit a plethora of applications in nanomedicine and oncology.

Acknowledgments

The authors acknowledge the financial support from the following Brazilian research agencies: Coordenação de Aperfeiçoamento de Pessoal de Nível Superior (PROEX-433/2010; PNPD), Fundação de Amparo à Pesquisa do Estado de Minas Gerais (PPM-00202-13; BCN-TEC 30030/12), Conselho Nacional de Pesquisa (PQ1B–306306/2014-0; UNIVERSAL-457537/2014-0), and Financiadora de Estudos e Projetos (CTINFRA-PROINFRA 2008/2010). The authors express their gratitude to the staff of the Microscopy Center at UFMG for their assistance with TEM–energy dispersive X-ray analysis. Finally, the authors thank the staff of the Center of Nanoscience, Nanotechnology and Innovation–CeNano²I/CEMUCASI/UFMG for the spectroscopy analyses.

Disclosure

The authors report no conflicts of interest in this work.

References

1. Nel AE, Mädler L, Velegol D, et al. Understanding biophysicochemical interactions at the nano–bio interface. *Nat Mater*. 2009;8(7):543–557.
2. Nel A, Xia T, Mädler L, Li N. Toxic potential of materials at the nanolevel. *Science*. 2006;311(5761):622–627.
3. Mansur HS, Mansur AAP, Soriano-Araújo A, Lobato ZIP. Beyond biocompatibility: an approach for the synthesis of ZnS quantum dot-chitosan nano-immunoconjugates for cancer diagnosis. *Green Chem*. 2015;17:1820–1830.
4. Srivastava V, Gusain D, Sharma YC. Critical review on the toxicity of some widely used engineered nanoparticles. *Ind Eng Chem Res*. 2015;54(2):6209–6233.
5. Tsoi K, Dai Q. Are quantum dots toxic? Exploring the discrepancy between cell culture and animal studies. *Acc Chem Res*. 2013;46(3):662–671.
6. Hauck TS, Anderson RE, Fischer HC, Newbigging S, Chan WCW. In vivo quantum-dot toxicity assessment. *Small*. 2010;6(1):138–144.
7. Yong K-T, Law W-C, Hu R, et al. Nanotoxicity assessment of quantum dots: from cellular to primate studies. *Chem Soc Rev*. 2013;42(3):1236–1250.
8. Ye L, Yong K, Liu L, et al. A pilot study in non-human primates shows no adverse response to intravenous injection of quantum dots. *Nature Nanotech*. 2012;7(7):453–458.
9. Oh E, Liu R, Nel A, et al. Meta-analysis of cellular toxicity for cadmium-containing quantum dots. *Nature Nanotech*. 2016;11(5):479–486.
10. Geraci C, Heidel D, Sayes C, et al. Perspectives on the design of safer nanomaterials and manufacturing processes. *J Nanopart Res*. 2015;17(9):366.
11. Wang Y, Santos A, Evdokiou A, Losic D. An overview of nanotoxicity and nanomedicine research: principles, progress and implications for cancer therapy. *J Mater Chem B*. 2015;3:7153–7172.
12. Tan WB, Huang N, Zhang Y. Ultrafine biocompatible chitosan nanoparticles encapsulating multi-coloured quantum dots for bioapplications. *J Colloid Interface Sci*. 2007;310(2):464–470.
13. Yong K, Swihart MT. In vivo toxicity of quantum dots: no cause for concern? *Nanomedicine*. 2012;7(11):1641–1643.
14. Medintz IL, Uyeda HT, Goldman ER, Mattoussi H. Quantum dot bioconjugates for imaging, labelling and sensing. *Nat Mater*. 2005;4(6):435–446.
15. Mansur HS, Mansur AAP, Curti E, de Almeida MV. Bioconjugation of quantum-dots with chitosan and N,N,N-trimethyl chitosan. *Carbohyd Polym*. 2012;90(1):189–196.
16. Sun XL, Cui W, Haller C, Chaikof EL. Site-specific multivalent carbohydrate labeling of quantum dots and magnetic beads. *Chembiochem*. 2004;5(11):1593–1596.
17. Mansur AAP, de Carvalho SM, Mansur HS. Bioengineered quantum dot/chitosan-tripeptide nanoconjugates for targeting the receptors of cancer cells. *Int J Biol Macromol*. 2016;82:780–789.
18. Mansur AAP, Saliba JB, Mansur HS. Surface modified fluorescent quantum dots with neurotransmitter ligands for potential targeting of cell signaling applications. *Colloids Surf B*. 2013;111:60–70.
19. Mansur AAP, Mansur HS, González J. Enzyme-polymers conjugated to quantum-dots for sensing applications. *Sensors*. 2011;11(10):9951–9972.
20. Sperling RA, Parak WJ. Surface modification, functionalization and bioconjugation of colloidal inorganic nanoparticles. *Philos Trans A Math Phys Eng Sci*. 2010;368(1915):1333–1383.
21. Upadhyaya L, Agarwal JSV, Tewari RP. Biomedical applications of carboxymethyl chitosans. *Carbohyd Polym*. 2013;91(1):452–466.
22. Shao L, Gao Y, Yan F. Semiconductor quantum dots for biomedicial applications. *Sensors*. 2011;11(12):11736–11751.
23. Brunetti V, Chibli H, Fiammengo R, et al. InP/ZnS as a safer alternative to CdSe/ZnS core/shell quantum dots: in vitro and in vivo toxicity assessment. *Nanoscale*. 2013;5(1):307–317.
24. Eaton DF. Reference materials for fluorescence. *Pure Appl Chem*. 1988;60:1107–1114.
25. Rajeshwar K, de Tacconi NR, Chenthamarakshan CR. Semiconductor-based composite materials: preparation, properties, and performance. *Chem Mater*. 2001;13:2765–2782.

26. Tauc J, Menth A. States in the gap. *J Non Cryst Solids*. 1972;8–10: 569–585.
27. Spanhel L, Haase M, Weller H, Henglein A. Photochemistry of colloidal semiconductor. *J Am Chem Soc*. 1987;109:5649–5655.
28. Jaiswal A, Sanpui P, Chattopadhyay A, Ghosh SS. Investigating fluorescence quenching of ZnS quantum dots by silver nanoparticles. *Plasmonics*. 2011;6:125–132.
29. Veamatahau A, Jiang B, Seifert T, et al. Origin of surface trap states in CdS quantum dots: relationship between size dependent photoluminescence and sulfur vacancy trap states. *Phys Chem Chem Phys*. 2015; 17(4):2850–2858.
30. Chen R, Li D, Liu B, et al. Optical and excitonic properties of crystalline ZnS nanowires: toward efficient ultraviolet emission at room temperature. *Nano Lett*. 2010;10(12):4956–4961.
31. Mansur HS. Quantum dots and nanocomposites. *Wiley Interdiscip Rev Nanomed Nanobiotechnol*. 2010;2(2):113–129.
32. Ghazzal MN, Wojcieszak R, Raj G, Gaigneaux EM. Study of mesoporous CdS-quantum-dot-sensitized TiO_2 films by using X-ray photoelectron spectroscopy and AFM. *Beilstein J Nanotechnol*. 2014;5: 68–76.
33. Moulder JF, Stickle WF, Sobol PE, Bomben KD. In: Chastain J, editor. *Handbook of X-Ray Photoelectron Spectroscopy*. Eden Prairie, MN: Perkin-Elmer Corporation; 1992.
34. Barreca D, Gasparotto A, Maragno C, Tondello E, Spalding TR. Analysis of nanocrystalline ZnS thin films by XPS. *Surf Sci Spectra*. 2002;9: 51–64.
35. López MC, Espinos JP, Martín F, Leinen D, Ramos-Barrado JR. Growth of ZnS thin films obtained by chemical spray pyrolysis: the influence of precursors. *J Cryst Growth*. 2008;285:66–75.
36. Williams NJ, Gan W, Reibenspies JH, Hancock RD. Possible steric control of the relative strength of chelation enhanced fluorescence for zinc (II) compared to cadmium (II): metal Ion complexing properties of tris(2-quinolylmethyl)amine, a crystallographic, UV-visible, and fluorometric study. *Inorg Chem*. 2009;48(4):1407–1415.
37. Mansur HS, Mansur AAP, Curti E, de Almeida MV. Functionalized-chitosan/quantum dot nano-hybrids for nanomedicine applications: towards biolabeling and biosorbing phosphate metabolites. *J Mater Chem B*. 2013;1:1696–1711.
38. Mansur HS, Mansur AAP, Ramanery FP, Borsagli FGLM. Green and facile synthesis of water-soluble ZnS quantum dots nanohybrids using chitosan derivative ligands. *J Nanopart Res*. 2014;16:1–14.
39. Raju GSR, Pavitra E, Nagaraju GP, Ramesh K, El-Rayes BF, Yu JS. Imaging and curcumin delivery in pancreatic cancer cell lines using PEGylated α-$Gd_2(MoO_4)_3$ mesoporous particles. *Dalton Trans*. 2014; 43(8):3330–3338.
40. Choi HS, Liu W, Misra P, et al. Renal clearance of quantum dots. *Nat Biotechnol*. 2007;25:1165–1170.
41. Beck-Broichsitter M, Ruppert C, Schmehl T, et al. Biophysical investigation of pulmonary surfactant surface properties upon contact with polymeric nanoparticles in vitro. *Nanomedicine*. 2015;7(3):341–350.
42. Cho SJ, Maysinger D, Jain M, Roder B, Hackbarth S, Winnik FM. Long-term exposure to CdTe quantum dots causes functional impairments in live cells. *Langmuir*. 2007;23(4):1974–1980.
43. Li KG, Chen JT, Bai SS, et al. Intracellular oxidative stress and cadmium ions release induce cytotoxicity of unmodified cadmium sulfide quantum dots. *Toxicol In Vitro*. 2009;23(6):1007–1013.
44. See V, Free P, Cesbron Y, et al. Cathepsin L digestion of nanobioconjugates upon endocytosis. *ACS Nano*. 2009;3(9):2461–2468.
45. Fischer HC, Hauck TS, Gomez-Aristizabal A, Chan WCW. Exploring primary liver macrophages for studying quantum dot interactions with biological systems. *Adv Mater*. 2010;22(23):2520–2524.
46. Albanese A, Tang PS, Chan WC. The effect of nanoparticle size, shape, and surface chemistry on biological systems. *Annu Rev Biomed Eng*. 2012;14:1–16.
47. Poulsen CB, Borup R, Borregaard N, Nielsen FC, Møller MB, Ralfkiaer E. Prognostic significance of metallothionein in B-cell lymphomas. *Blood*. 2006;108(10):3514–3519.
48. Waalkes MP. Cadmium carcinogenesis. *Mutat Res Fundam Mol Mech Mutagen*. 2003;533(1–2):107–120.
49. Nielsen AE, Bohr A, Penkowa M. The balance between life and death of cells: roles of metallothioneins. *Biomark Insights*. 2006;1:99–111.
50. Tokar EJ, Benbrahim-Tallaa L, Waalkes MP. Metal ions in human cancer development. *Met Ions Life Sci*. 2011;8:375–401.
51. Gladkovskaya O, Greaney P, Gun'ko YK, O'Connor GM, Meerec M, Rochev Y. An experimental and theoretical assessment of quantum dot cytotoxicity. *Toxicol Res*. 2015;4:1409–1415.
52. Nguyena KC, Willmoreb WG, Tayabalia AF. Cadmium telluride quantum dots cause oxidative stress leading to extrinsic and intrinsic apoptosis in hepatocellular carcinoma HepG2 cells. *Toxicology*. 2013; 306:114–123.
53. Duan H, Nie S. Cell-penetrating quantum dots based on multivalent and endosome-disrupting surface coatings. *J Am Chem Soc*. 2007;129(11): 3333–3338.
54. Clift MJD, Stone V. Quantum dots: an insight and perspective of their biological interaction and how this relates to their relevance for clinical use. *Theranostics*. 2012;2(7):668–680.
55. Marsh M, McMahon HT. The structural era of endocytosis. *Science*. 1999;285(5425):215–220.
56. Kim TK, Eberwine JH. Mammalian cell transfection: the present and the future. *Anal Bioanal Chem*. 2010;397(8):3173–3178.
57. Salgado CL, Mansur AAP, Mansur HS, Monteiro FJM. Fluorescent bionanoprobes based on quantum dot-chitosan–O-phospho-L-serine conjugates for labeling human bone marrow stromal cells. *RSC Adv*. 2014;4:49016–49027.
58. Wang T, Bai J, Jiang X, Nienhaus GU. Cellular uptake of nanoparticles by membrane penetration: a study combining confocal microscopy with FTIR spectroelectrochemistry. *ACS Nano*. 2012;6(2):1251–1259.